

Electronic Supplementary Information

Revisiting indeno[2,1-*c*]fluorene synthesis while exploring the fully conjugated *s*-indaceno[2,1-*c*:6,5-*c'*]difluorene

Himanshu Sharma,^a Priyank Kumar Sharma,^a and Soumyajit Das* ^a

^aDepartment of Chemistry, Indian Institute of Technology Ropar, Nangal Road, Rupnagar, Punjab-140001, India. E-mail: chmsdas@iitrpr.ac.in

Table of Contents

1.	Indacenodifluorene Isomers	S2
2.	Experimental Section.....	S2
2.1	General Information and Syntheses.....	S2
2.2	NMR Spectra.....	S8
3.	DFT Calculations.....	S19
3.1	TD-DFT Calculations.....	S20
3.2	Frontier Molecular Orbitals.....	S22
3.3	NICS(1)zz and HOMA Indices	S23
4.	Single Crystal Data.....	S24
5.	References.....	S31

1. Indacenodifluorene Isomers

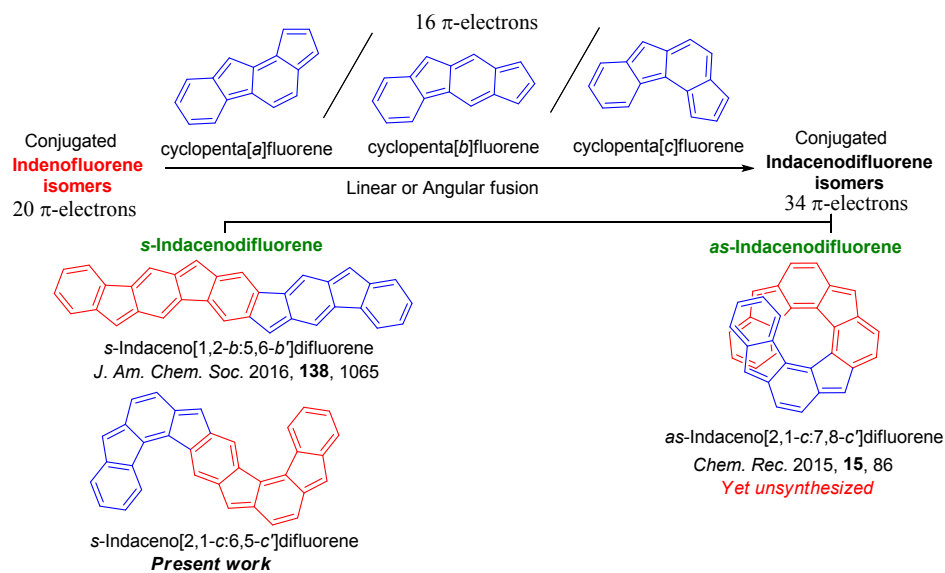


Fig. S1 Known indacenodifluorene (IDF) isomers with 34π -electrons delocalized along the conjugated backbone.

2. Experimental Section

2.1 General Information and Syntheses: Chemicals and reagents were purchased from commercial suppliers (Merck, GLR innovations, BLDpharm) and used without further purification. Thin layer chromatography (TLC) was performed using pre-coated plates purchased from Merck (silica gel 60 PF254, 0.25 mm). Column chromatography was performed using silica gel 100-200 mesh. NMR spectra were recorded in CDCl_3 and C_6D_6 (Eurisotop) at 298 K, on JEOL JNM-ECS400 spectrometer at operating frequencies of 400 MHz (^1H) or 100 MHz (^{13}C) as indicated in the individual spectrum. Chemical shifts (δ) are given in ppm relative to residual solvent (chloroform $\delta = 7.26$, benzene $\delta = 7.16$, 1,1,2,2-tetrachloroethane $\delta = 6.00$ for ^1H , and chloroform $\delta = 77.16$ for proton decoupled ^{13}C NMR) and coupling constants (J) in Hz. Multiplicity is tabulated as s for singlet, d for doublet, dd for doublet of doublet, t for triplet, q for quartet and m for multiplet. High resolution mass spectra (HRMS) were recorded using electron spray ionization (ESI) methods on Waters (XEVO G2-XS QTOF) mass spectrometer. UV-vis-NIR spectrum of **4** was recorded in JASCO V-670 spectrophotometer. Cyclic voltammetry of **4** was performed in CH instruments using dry dichloromethane/TBAPF₆ solvent/electrolyte couple at a scan rate of 50 mV/s. Melting points were determined using BIBBY-SMP30 melting point analyzer. Single crystal X-ray structural data were collected on a

CMOS based Bruker D8 Venture PHOTON 100 diffractometer equipped with a INCOATEC micro-focus source with graphite monochromated Mo K α radiation ($\lambda = 0.71073 \text{ \AA}$) operating at 50 kV and 30 mA.

2'-bromo-[1,1'-biphenyl]-2-carbaldehyde (7): An oven-dried thick-walled glass tube was charged with **5** (1 g, 3.53 mmol), 2-formylphenylboronic acid **6** (583 mg, 3.86 mmol), anhydrous K₂CO₃ (2.44 g, 17.67 mmol), dry toluene (5 mL), and purged with nitrogen for 30 mins. The vial was sealed under nitrogen after adding PdCl₂(dppf)·DCM complex (144 mg, 0.18 mmol), and the mixture was warmed at 100 °C for 12 h. After being cooled to room temperature, water was added and the resultant mixture was extracted with DCM (3 x 50 mL). The organic layer was dried over anhydrous Na₂SO₄, filtered, and evaporated under reduced pressure to afford a crude residue which was column chromatographed on silica gel (hexanes:EtOAc, 95:5) to afford the title product **7** as light yellow viscous oil (664 mg, 72% yield). $R_f = 0.45$ (hexanes:EtOAc = 20:1). ¹H NMR (400 MHz, CDCl₃): δ 9.74 (s, 1H), 7.99 (d, $J = 7.7 \text{ Hz}$, 1H), 7.67–7.59 (m, 2H), 7.50 (t, $J = 7.5 \text{ Hz}$, 1H), 7.37 (t, $J = 7.4 \text{ Hz}$, 1H), 7.31–7.21 (m, 3H). ¹³C{¹H} NMR (100 MHz, CDCl₃): δ 191.7, 144.6, 138.9, 133.8, 133.7, 132.8, 131.7, 130.9, 129.9, 128.6, 127.5, 127.4, 123.9. HRMS (ESI) *m/z*: [M + H]⁺ Calcd for C₁₃H₁₀OB_r 260.9915, found 260.9902.

4-bromo-9-mesityl-9*H*-fluorene (10): 2-Mesylmagnesium bromide (1 M solution in THF, 4.98 mL, 4.98 mmol) was added dropwise to the 10 mL dry THF solution of compound **7** (650 mg, 2.49 mmol) under nitrogen, and the mixture was stirred at room temperature for 24 h. The reaction mixture was quenched with saturated solution of ammonium chloride (50 mL), and the volatile organics were evaporated *in vacuo*. The residue was extracted with DCM (3 x 50 mL), washed with water, and dried over sodium sulfate. The organic layer was filtered, and the filtrate was removed under reduced pressure to afford crude **9** as yellow solid (1.2 g). To the solution of crude **9** (1.2 g) in anhydrous DCM (10 mL) at room temperature, BF₃·Et₂O (0.1 mL) was added dropwise under nitrogen, and the reaction mixture was stirred for 10 min at room temperature to perform an intra-molecular ring-closure reaction. After 10 min, a saturated aqueous NH₄Cl solution was added to the reaction mixture and it was extracted with DCM (3 x 50 mL). The organic layer was dried over anhydrous Na₂SO₄, filtered, and removed under reduced pressure to afford a residue which was purified by silica gel column chromatography (hexanes) to give **10** as white solid (655 mg, 72% yield in two steps). $R_f = 0.47$ (hexanes). mp: 108–109 °C. ¹H NMR (400 MHz, CDCl₃): δ 8.66 (d, $J = 7.8 \text{ Hz}$, 1H), 7.54 (d, $J = 7.7 \text{ Hz}$, 1H), 7.44 (t, $J = 7.5 \text{ Hz}$, 1H),

7.31 (t, J = 7.4 Hz, 1H), 7.21 (d, J = 7.4 Hz, 1H), 7.15 (d, J = 7.3 Hz, 1H), 7.08 (t, J = 7.6 Hz, 1H), 7.02 (s, 1H), 6.66 (s, 1H) 5.48 (s, 1H), 2.65 (s, 3H), 2.28 (s, 3H), 1.08 (s, 3H). $^{13}\text{C}\{\text{H}\}$ NMR (100 MHz, CDCl_3): δ 150.2, 147.7, 140.2, 139.1, 137.8, 137.8, 136.6, 133.5, 131.9, 130.7, 129.0, 128.0, 127.9, 126.7, 123.9, 123.7, 123.0, 117.2, 49.9, 29.8, 21.8, 21.0, 18.9. HRMS (ESI) m/z : [M - H]⁺ Calcd for $\text{C}_{22}\text{H}_{18}\text{Br}$ 361.0592, found 361.0593.

2-(9-mesityl-9*H*-fluoren-4-yl)benzaldehyde (11**):** An oven-dried thick-walled glass tube was charged with **10** (125 mg, 0.344 mmol), **6** (103.18 mg, 0.688 mmol), anhydrous K_2CO_3 (237.76 mg, 1.72 mmol), dry toluene (6 mL) and purged with nitrogen for 30 min. Catalyst $\text{PdCl}_2(\text{dppf})\cdot\text{DCM}$ complex (28.09 mg, 10 mol%) was added subsequently under nitrogen, and the glass tube was sealed. The reaction mixture was then warmed at 90 °C for 12 h. After being cooled to room temperature, the mixture was washed with water and extracted with DCM (3 x 50 mL). The DCM layer was dried over anhydrous Na_2SO_4 , filtered, and removed under vacuum. The crude residue was purified by silica gel column chromatography (hexanes:DCM, 52:48) to afford the desired compound **11** as white solid (112 mg, 84% yield). R_f = 0.30 (hexanes:DCM = 10:3). **mp:** 173–174 °C. ^1H NMR (400 MHz, CDCl_3): δ 9.88–9.79 (m, 1H), 8.15 (d, J = 7.7 Hz, 1H), 7.76 (t, J = 7.4 Hz, 1H), 7.65 (t, J = 7.6 Hz, 1H), 7.58–7.46 (m, 1H), 7.37–7.27 (m, 2H), 7.25–7.07 (m, 3H), 7.06–6.91 (m, 2H), 6.68 (s, 1H), 6.55 (dd, J = 7.7, 3.2 Hz, 1H), 5.54 (s, 1H), 2.70 (m, 3H), 2.29 (s, 3H), 1.14–1.13 (m, 3H). $^{13}\text{C}\{\text{H}\}$ NMR (100 MHz, CDCl_3): δ 192.3, 192.0, 147.9, 147.9, 147.8, 144.9, 140.1, 139.1, 139.0, 137.9, 137.8, 137.7, 136.6, 136.5, 134.3, 134.2, 134.1, 133.7, 132.6, 131.0, 130.8, 130.6, 129.4, 129.2, 129.1, 129.0, 128.6, 127.4, 127.4, 127.4, 126.9, 126.8, 124.2, 124.1, 124.1, 122.4, 49.7, 29.8, 21.9, 21.0, 18.8, 18.8. HRMS (ESI) m/z : [M + H]⁺ Calcd for $\text{C}_{29}\text{H}_{25}\text{O}$ 389.1905, found 389.1898.

5,8-dimesityl-5,8-dihydroindeno[2,1-*c*]fluorene (13**):** 2-Mesilylmagnesium bromide (1.0 M in THF, 0.50 mL, 0.50 mmol) was added dropwise to the dry THF solution of **11** (98 mg, 0.25 mmol) under nitrogen atmosphere. The mixture was stirred at room temperature for 24 h, and then quenched by saturated aqueous NH_4Cl solution and extracted with DCM (3 x 50 mL). The organic layer was dried over anhydrous Na_2SO_4 and the solvent was removed under reduced pressure to afford crude product **12** as yellow solid (146 mg, HRMS m/z : [M - H]⁺ Calcd for $\text{C}_{38}\text{H}_{35}\text{O}$ 507.2688, found 507.2691). To the solution of crude **12** (141 mg, 0.277 mmol) in anhydrous DCM (10 mL) at room temperature, $\text{BF}_3\cdot\text{Et}_2\text{O}$ (0.1 mL) was added dropwise under nitrogen, and the reaction mixture was stirred for 10 min at room temperature. Progress of the

intra-molecular ring-closure reaction was monitored by TLC. As the starting material disappeared, a saturated aqueous NH₄Cl solution was added to the reaction mixture and extracted with DCM. The organic layer was dried over anhydrous Na₂SO₄, filtered, and the solvent was subsequently removed under reduced pressure. The residue was purified by silica gel column chromatography (hexanes:DCM, 92:8) to afford dihydro precursor **13** as mixture of diastereomers, as white solid (69 mg, 56% yield in two steps). R_f = 0.50 (hexanes:DCM = 10:1). **mp:** 204–205 °C. **¹H NMR** (400 MHz, CDCl₃): δ 8.64 (dd, J = 16.1, 7.9 Hz, 2H), 7.55–7.47 (m, 2H), 7.37–7.27 (m, 4H), 7.06 (d, J = 7.9 Hz, 2H), 7.02 (s, 2H), 6.64 (d, J = 11.4 Hz, 2H), 5.58 (d, J = 9.2 Hz, 2H), 2.69 (s, 3H), 2.68 (s, 3H), 2.28 (s, 3H), 2.27 (s, 3H), 1.09 (s, 3H), 1.05 (s, 3H). **¹³C{¹H} NMR** (100 MHz, CDCl₃): δ 148.5, 148.4, 148.1, 147.5, 141.5, 141.3, 137.9, 137.8, 136.4, 136.3, 136.2, 134.6, 134.5, 130.7, 128.9, 127.1, 126.7, 124.5, 124.4, 123.9, 123.7, 122.8, 122.5, 50.0, 29.8, 21.9, 21.0, 20.9, 18.8, 18.6. **HRMS** (ESI) *m/z*: [M + H]⁺ Calcd for C₃₈H₃₅ 491.2739, found 491.2710.

5,8-dimesitylindeno[2,1-*c*]fluorene (3): Precursor **13** (44 mg, 0.089 mmol) was dissolved in dry toluene (1 mL) and purged with nitrogen for 10 mins. DDQ (26.5 mg, 0.116 mmol, 1.3 equiv) as solid was added into the solution, and the reaction mixture was warmed to 90 °C for 2 h while the progress was monitored by TLC. After 2 h, the solvent was removed by vacuum and the crude residue was purified by silica gel column chromatography (hexanes) to afford the final compound **3** as green solid (42 mg, 96% yield). R_f = 0.27 (hexanes). **mp:** 182–183 °C. **¹H NMR** (400 MHz, CDCl₃): δ 8.10 (d, J = 7.4 Hz, 2H), 7.14 (t, J = 7.4 Hz, 2H), 7.07 (t, J = 7.4 Hz, 2H), 6.96 (s, 4H), 6.69 (d, J = 7.2 Hz, 2H), 6.11 (s, 2H), 2.35 (s, 6H), 2.14 (s, 12H). **¹³C{¹H} NMR** (100 MHz, CDCl₃): δ 146.2, 143.4, 138.9, 137.5, 137.1, 136.4, 130.0, 129.2, 128.2, 126.6, 125.5, 121.8, 121.0, 21.3, 20.4. **HRMS** (ESI) *m/z*: [M]⁺ Calcd for C₃₈H₃₂ 488.2504, found 488.2496.

2-(9-mesityl-9*H*-fluoren-4-yl)-4,4,5,5-tetramethyl-1,3,2-dioxaborolane (15): An oven-dried glass tube was charged with **10** (400 mg, 1.10 mmol), bis(pinacolato)diboron (559.19 mg, 2.20 mmol), KOAc (324.17 mg, 3.30 mmol), dry 1,4-dioxane (5 mL). The suspension was purged with N₂ for 30 mins before adding PdCl₂(dppf)·DCM (89.83 mg, 10 mol%), and the glass tube was sealed. The reaction mixture was stirred at 85 °C for 3 h. After being cooled to room temperature, volatile organics were removed under reduced pressure and water was added. The mixture was extracted with DCM (5 x 60 mL), dried over anhydrous Na₂SO₄, and filtered. The organic layer was removed under reduced pressure, and the crude obtained was quickly column

chromatographed on short silica gel pad (hexanes:DCM, 70:30) to afford the title product **15** as white solid (349 mg, 77% yield). R_f = 0.4 (hexanes:DCM = 5:1). **mp:** 156–157 °C. **^1H NMR** (400 MHz, CDCl_3): δ 8.79 (d, J = 7.8 Hz, 1H), 7.86 (d, J = 7.2 Hz, 1H), 7.39 (t, J = 7.4 Hz, 1H), 7.28 (t, J = 7.3 Hz, 1H), 7.25–7.19 (m, 3H), 7.02 (s, 1H), 6.65 (s, 1H), 5.43 (s, 1H), 2.67 (s, 3H), 2.28 (s, 3H), 1.50 (s, 6H), 1.48 (s, 6H), 1.08 (s, 3H). **$^{13}\text{C}\{\text{H}\}$ NMR** (100 MHz, CDCl_3): δ 147.7, 147.4, 145.4, 142.0, 137.9, 137.8, 136.1, 134.9, 134.2, 130.5, 128.7, 127.0, 126.6, 126.0, 124.0, 123.7, 84.0, 49.5, 21.8, 20.9, 18.8. **HRMS** (ESI) m/z : [M + H]⁺ Calcd for $\text{C}_{28}\text{H}_{32}\text{O}_2\text{B}$ 411.2495, found 411.2489.

2,5-bis(9-mesityl-9*H*-fluoren-4-yl)terephthalaldehyde (17): An oven-dried glass tube was charged with compound **15** (298.71 mg, 0.727 mmol), 2,5-dibromophenyl-1,4-dialdehyde **16** (85 mg, 0.291 mmol), K_2CO_3 (201.20 mg, 1.46 mmol), tetrahydrofuran (10 mL) and water (1 mL), and the mixture was purged with nitrogen for 30 mins. Catalyst $\text{Pd}(\text{PPh}_3)_4$ (33.62 mg, 10 mol%) was subsequently added under nitrogen, and the glass tube was sealed before being warmed to 90 °C. After 12 h, the THF was evaporated under reduced pressure, and water was added. The mixture was extracted with DCM (4 x 50 mL), and the organic layer washed with saturated brine solution, and water. The organic layer was dried over anhydrous Na_2SO_4 , filtered, and removed under vacuum. The residue was purified by silica gel column chromatography (hexanes:DCM, 60:40) to afford the title product **17** as yellow solid (151 mg, 76% yield). R_f = 0.48 (hexanes:DCM = 20:7). **mp:** 318–319 °C. **^1H NMR** (400 MHz, CDCl_3): δ 10.03–9.93 (m, 2H), 8.31–8.29 (m, 2H), 7.44–7.31 (m, 6H), 7.25–6.93 (m, 10H), 6.73–6.71 (m, 2H), 5.60–5.59 (m, 2H), 2.73 (brs, 6H), 2.31 (brs, 6H), 1.20–1.16 (m, 6H). **$^{13}\text{C}\{\text{H}\}$ NMR:** (100 MHz, CDCl_3): δ 191.6, 191.4, 191.2, 148.3, 148.3, 148.3, 148.2, 148.2, 148.1, 148.1, 148.1, 148.1, 148.0, 144.5, 144.5, 144.4, 144.4, 144.3, 139.9, 139.9, 139.9, 139.8, 139.8, 139.1, 139.1, 139.1, 139.0, 139.0, 138.9, 137.9, 137.9, 137.8, 137.7, 137.6, 137.6, 137.5, 136.7, 136.7, 136.6, 133.6, 133.5, 133.5, 131.3, 131.2, 131.2, 130.8, 130.7, 130.4, 130.3, 130.2, 130.1, 130.1, 129.7, 129.6, 129.4, 129.2, 129.1, 129.0, 128.4, 128.3, 127.9, 127.7, 127.7, 127.3, 127.2, 127.0, 127.0, 126.9, 124.7, 124.6, 124.5, 122.2, 49.8, 49.8, 49.7, 29.8, 21.9, 21.0, 21.02, 19.1, 19.1, 18.9, 18.8, 18.8. **HRMS** (ESI) m/z : [M + H]⁺ Calcd for $\text{C}_{52}\text{H}_{43}\text{O}_2$ 699.3263, found 699.3244.

5,8,14,17-tetramesityl-5,8,14,17-tetrahydro-s-indaceno[2,1-*c*:6,5-*c'*]difluorene (19): 2-Mesitylmagnesium bromide (1.0 M in THF, 0.99 mL, 0.99 mmol) was added to the dry THF (5 mL) solution of **17** (139 mg, 0.198 mmol) under N_2 . The mixture was stirred at room

temperature for 24 h, and quenched with saturated aq. NH₄Cl solution. The volatile organics were evaporated, and the mixture was extracted with DCM (4 x 50 mL). The organic layer was dried over anhydrous Na₂SO₄, filtered, and removed under reduced pressure to afford crude tetracarbinol **18** (252 mg, HRMS (ESI) *m/z*: [M - H]⁺ Calcd for C₇₀H₆₅O₂ 937.4985, found 937.4962). To the solution of crude **18** (249 mg, 0.265 mmol) in anhydrous DCM (20 mL), BF₃·Et₂O (0.1 mL) was added dropwise under nitrogen and the reaction mixture was stirred for 10 min at room temperature. Once starting material **18** is consumed, as monitored by TLC, saturated aqueous NH₄Cl solution was added and the reaction mixture was extracted with DCM (4 x 50 mL). The organic layer was dried over anhydrous Na₂SO₄, filtered, and evaporated under reduced pressure. The residue was subjected to silica gel column chromatography (hexanes:DCM, 84:16), followed by trituration with methanol afforded off-white solid **19** (116 mg, 64% yield in two steps). **R**_f = 0.32 (hexanes:DCM = 10:1). **mp**: 288–289 °C. **¹H NMR** (400 MHz, CDCl₃): δ 8.50–8.04 (m, 4H), 7.39–7.28 (m, 2H), 7.24–7.02 (m, 12H), 6.79–6.58 (m, 4H), 5.83–5.73 (m, 2H), 5.59–5.54 (m, 2H), 2.89–2.67 (m, 12H), 2.38–2.21 (m, 12H), 1.18–0.99 (m, 12H). **¹³C{¹H} NMR**: (100 MHz, CDCl₃): δ 149.1, 148.5, 148.3, 147.5, 147.2, 141.4, 141.2, 140.1, 137.9, 137.8, 136.3, 134.9, 134.6, 130.8, 130.6, 129.2, 128.9, 126.9, 126.4, 124.3, 123.6, 122.9, 122.6, 122.2, 119.4, 119.2, 50.0, 29.8, 29.5, 21.9, 21.0, 19.2, 19.0, 18.8, 18.7, 15.98. HRMS (ESI) *m/z*: [M + H]⁺ Calcd for C₇₀H₆₃ 903.4930, found 903.4926.

5,8,14,17-tetramesityl-s-indaceno[2,1-*c*:6,5-*c'*]difluorene (4): DDQ (26.4 mg, 0.116 mmol, 2.1 equiv) was added to the **19** (50 mg, 0.055 mmol) in dry toluene (1 mL) under N₂, and the reaction mixture was warmed to 80 °C for 45 mins. Once the starting material was consumed (monitored by TLC), the toluene was removed *in vacuo* and the crude was purified by silica gel column chromatography (hexanes:DCM, 90:10) to afford the title product **4** as brown solid in quantitative yield. **R**_f = 0.4 (hexanes:DCM = 10:1). **mp**: > 390 °C. **¹H NMR** (400 MHz, C₆D₆): δ 7.85 (d, *J* = 7.6 Hz, 2H), 7.77 (s, 2H), 6.91 (s, 4H), 6.84 (s, 4H), 6.82 (t, *J* = 7.5 Hz, 2H), 6.73 (t, *J* = 7.5 Hz, 2H), 6.60 (d, *J* = 7.3 Hz, 2H), 6.31 (d, *J* = 9.2 Hz, 2H), 6.24 (d, *J* = 9.1 Hz, 2H), 2.25 (s, 12H), 2.23 (s, 6H), 2.19 (s, 6H), 2.14 (s, 12H). **¹H NMR** (400 MHz, C₂D₂Cl₄): δ 7.52 (d, *J* = 7.6 Hz, 2H), 7.27 (s, 2H), 7.06 (s, 4H), 7.01 (t, *J* = 7.5 Hz, 2H), 6.96 (s, 4H), 6.83 (t, *J* = 7.5 Hz, 2H), 6.65 (d, *J* = 7.4 Hz, 2H), 6.20 (d, *J* = 9.3 Hz, 2H), 6.09 (d, *J* = 9.2 Hz, 2H), 2.42 (s, 6H), 2.35 (s, 6H), 2.27 (s, 12H), 2.13 (s, 12H). Insufficient solubility did not allow ¹³C NMR study. HRMS (ESI) *m/z*: [M + H]⁺ Calcd for C₇₀H₅₉ 899.4617, found 899.4594.

2.2 NMR Spectra:

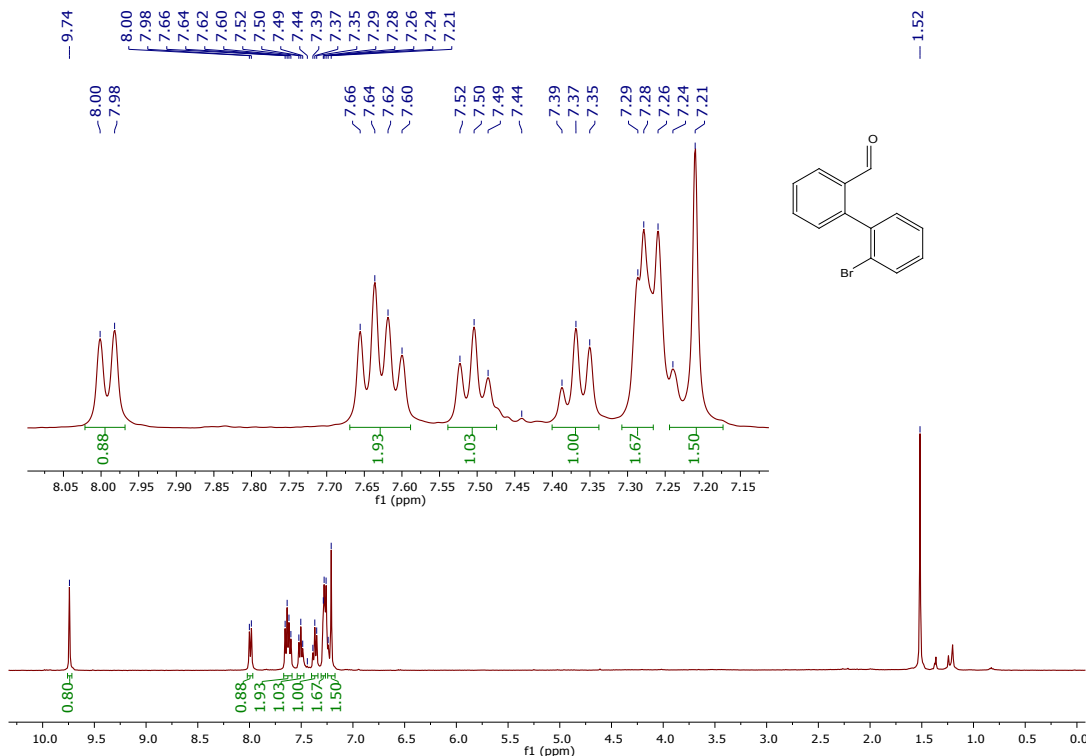


Fig. S2 ^1H NMR spectrum of **7** (in CDCl_3 , 400 MHz).

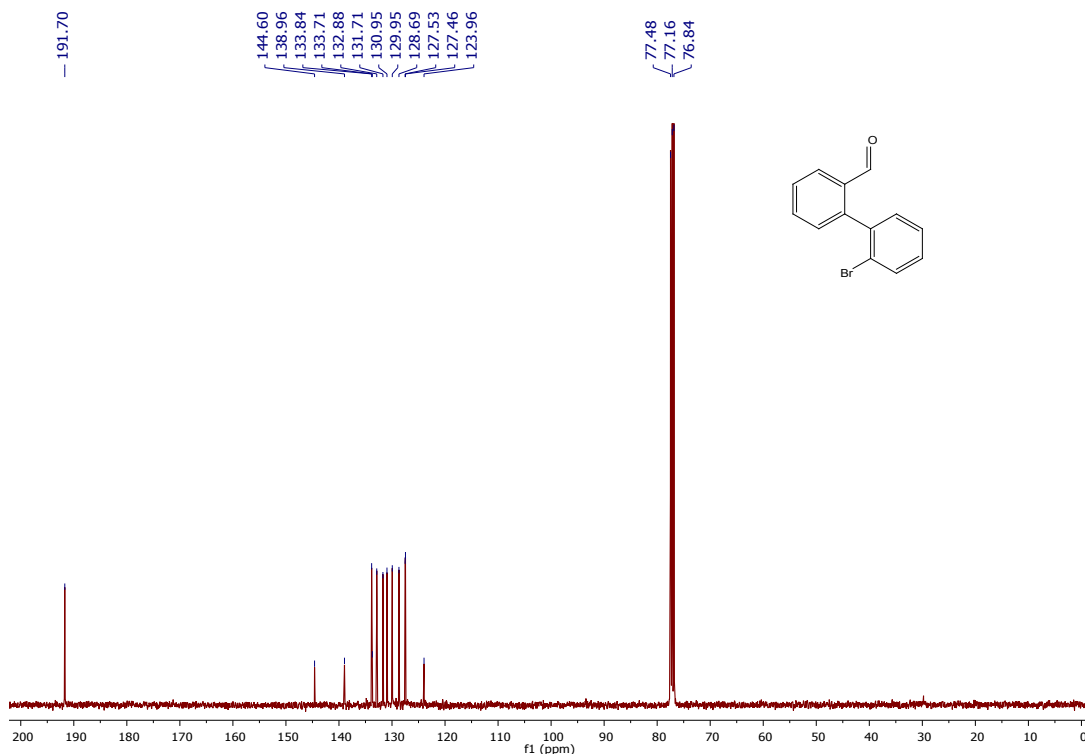


Fig. S3 ^{13}C NMR spectrum of **7** (in CDCl_3 , 100 MHz).

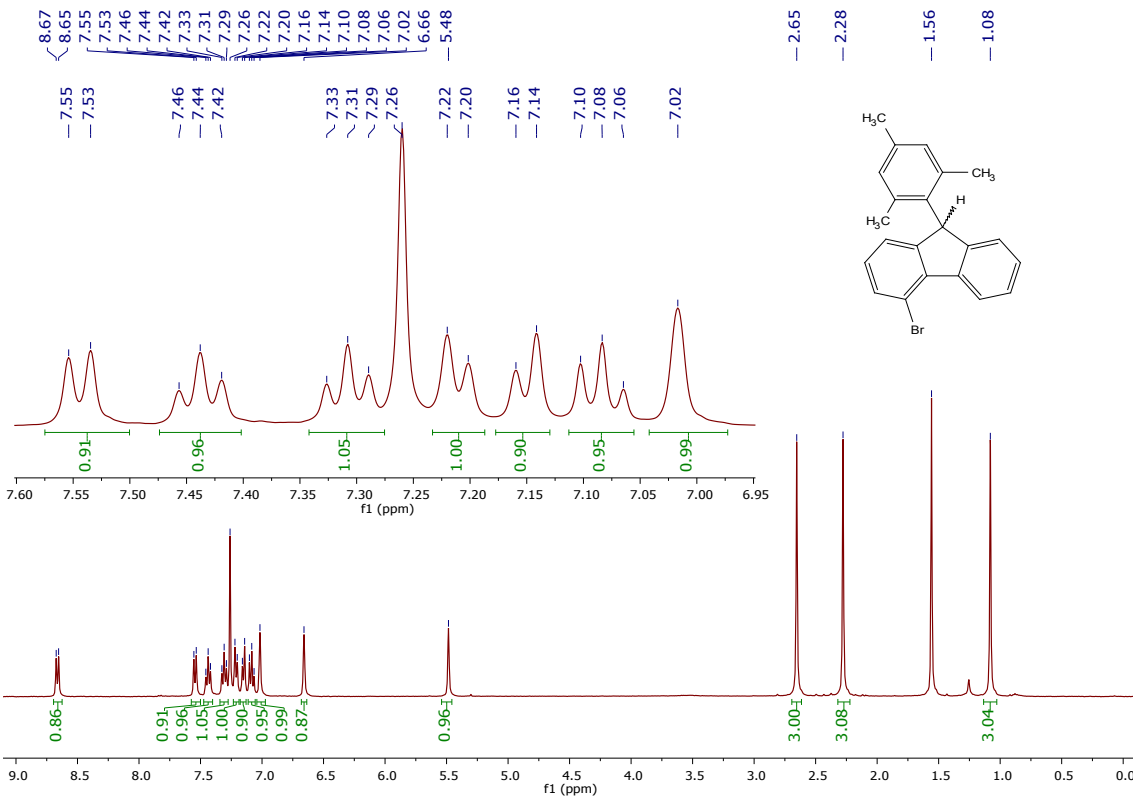


Fig. S4 ^1H NMR spectrum of **10** (in CDCl_3 , 400 MHz).

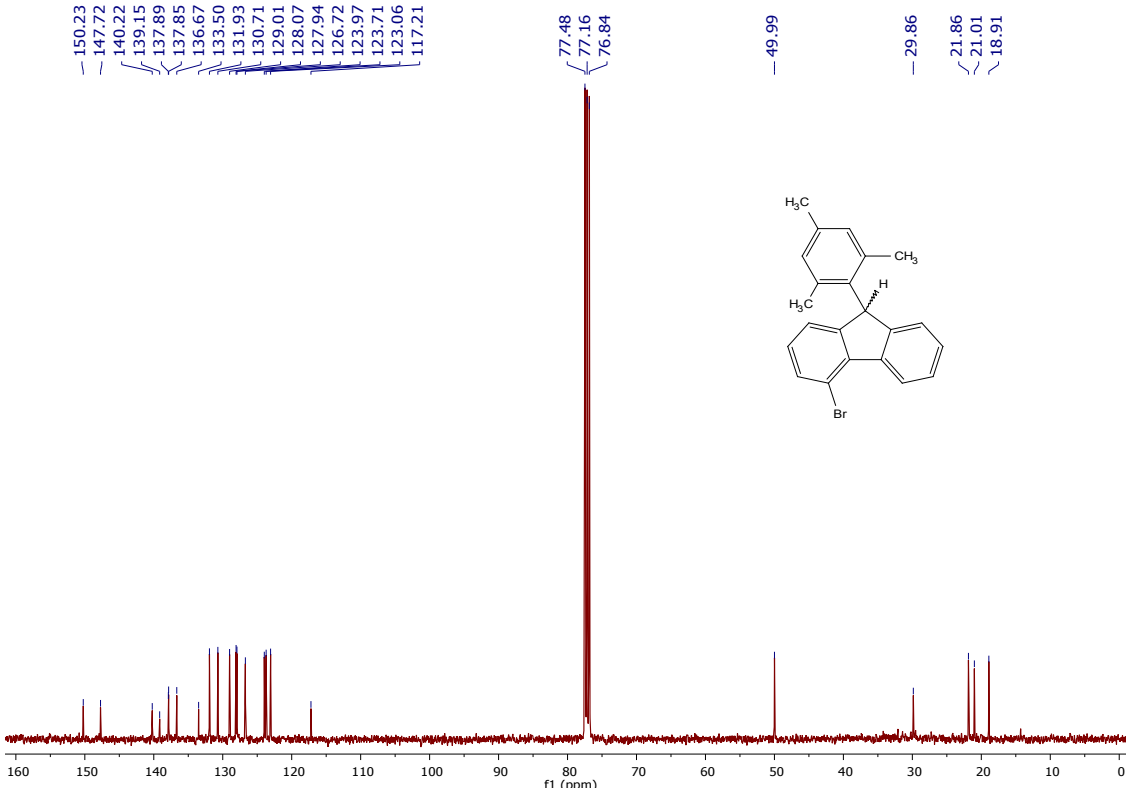
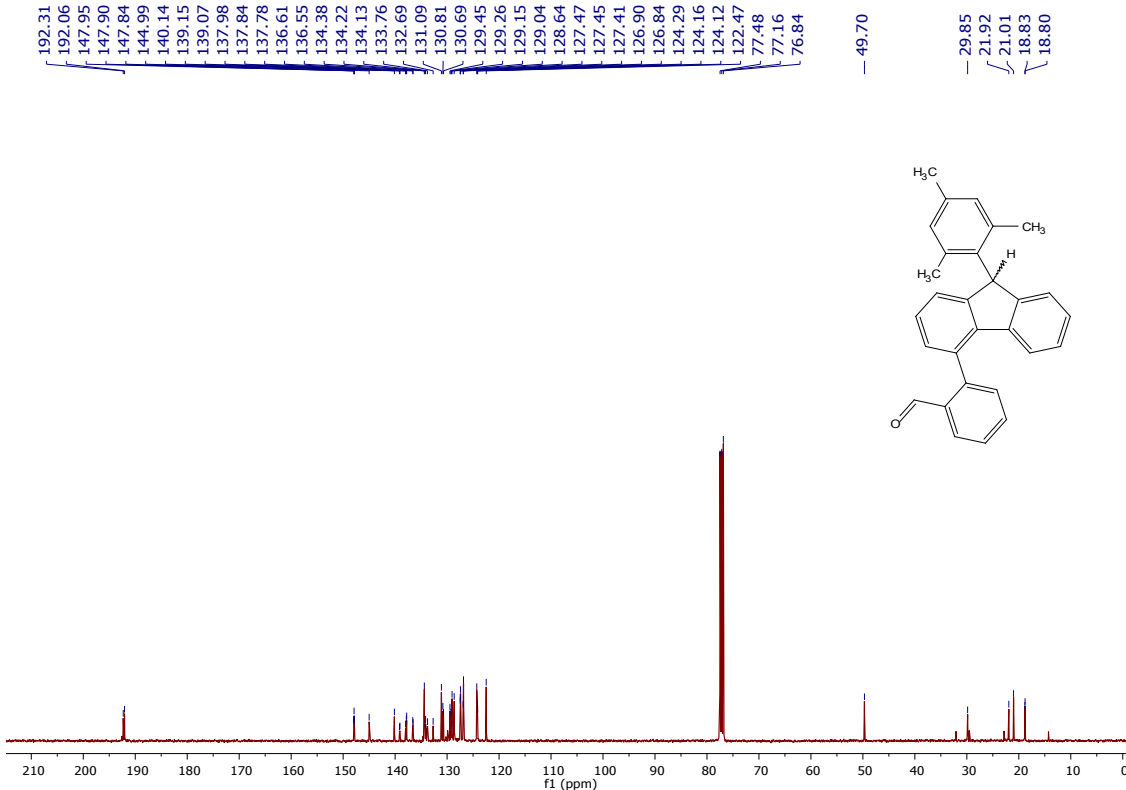
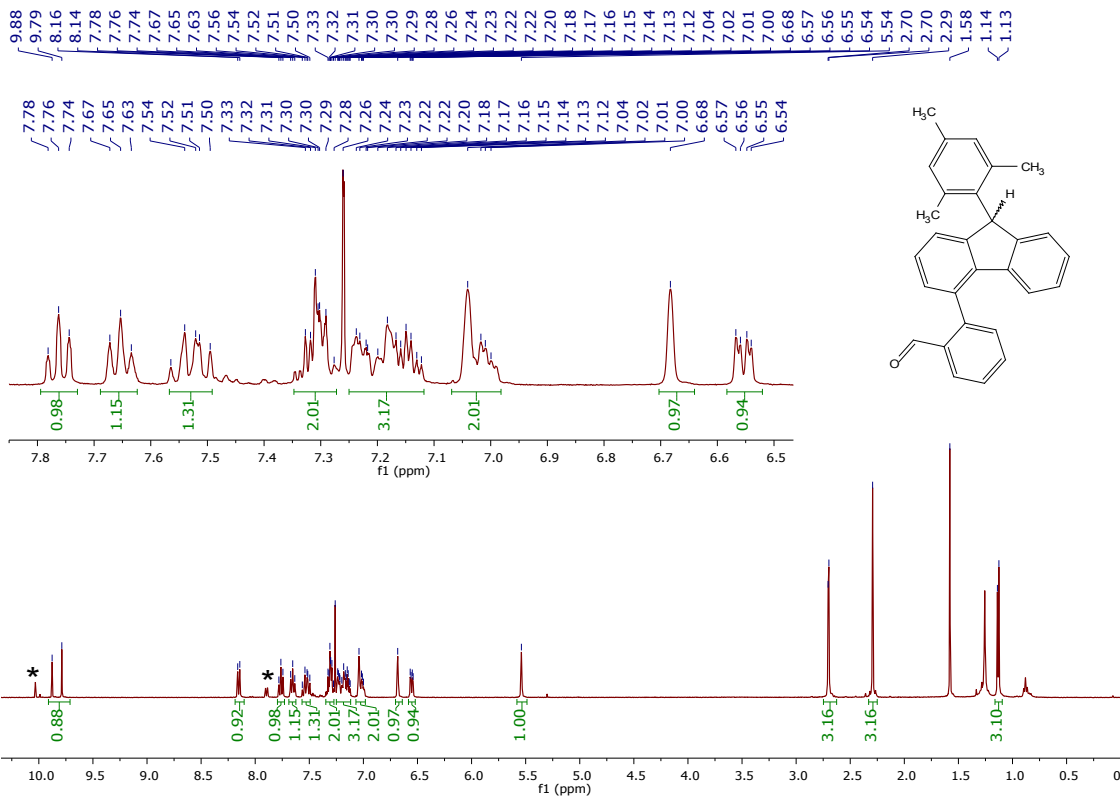


Fig. S5 ^{13}C NMR spectrum of **10** (in CDCl_3 , 100 MHz).



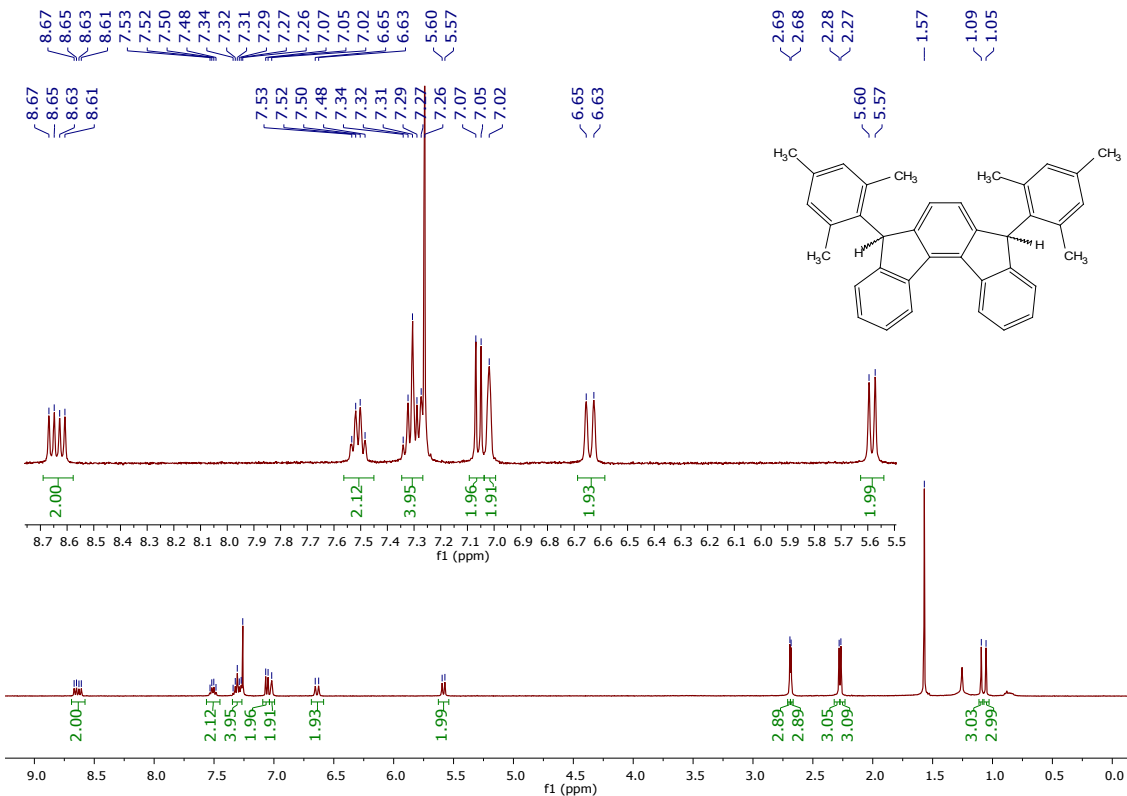


Fig. S8 ^1H NMR spectrum of **13** (in CDCl_3 , 400 MHz).

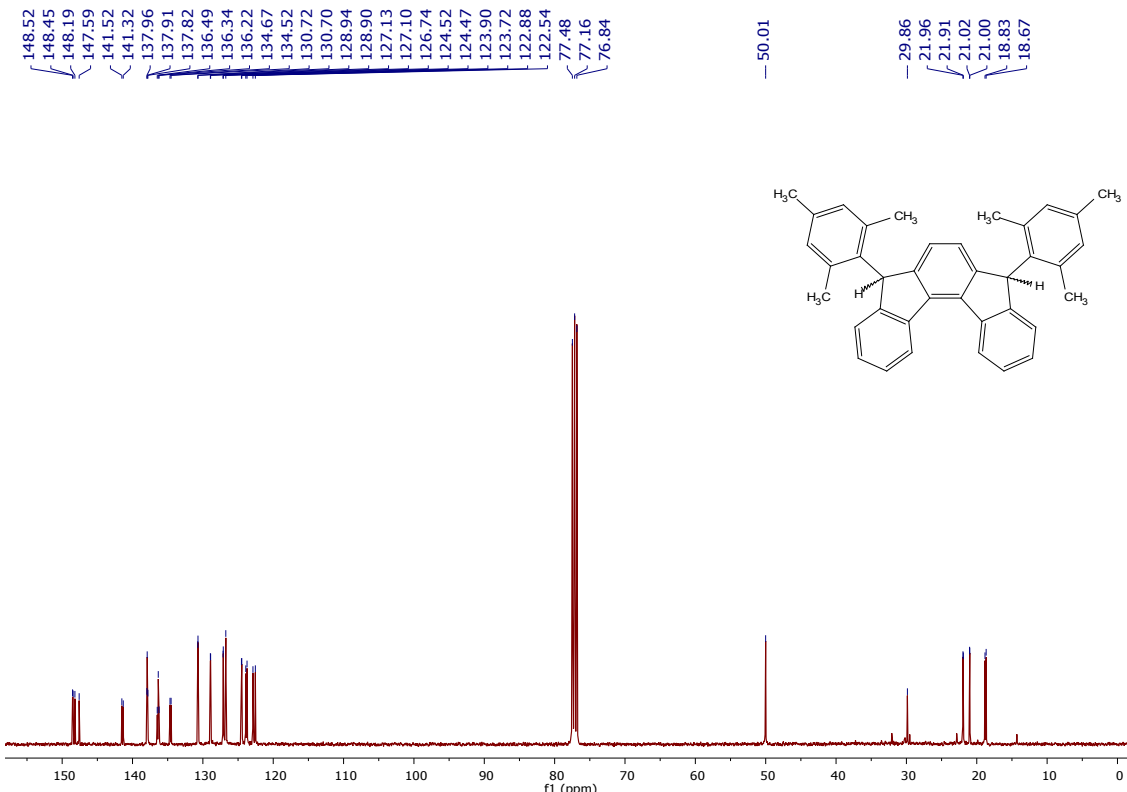


Fig. S9 ^{13}C NMR spectrum of **13** (in CDCl_3 , 100 MHz).

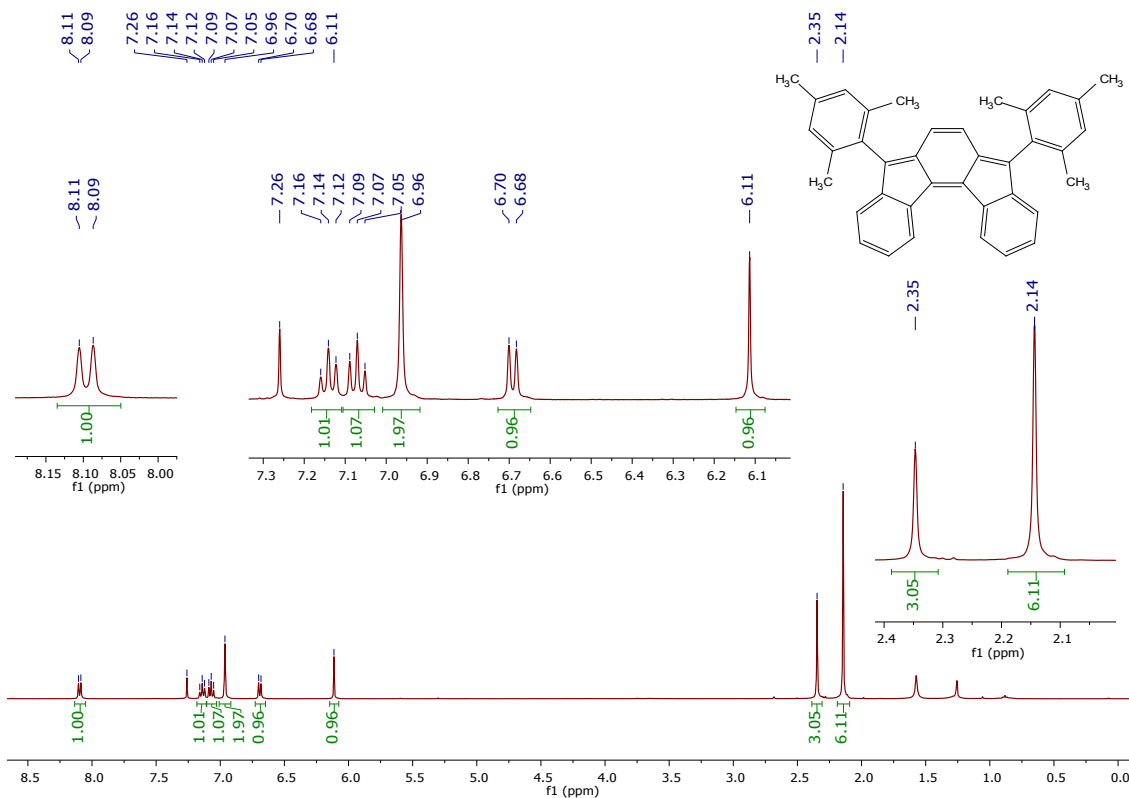


Fig. S10 ^1H NMR spectrum of **3** (in CDCl_3 , 400 MHz).

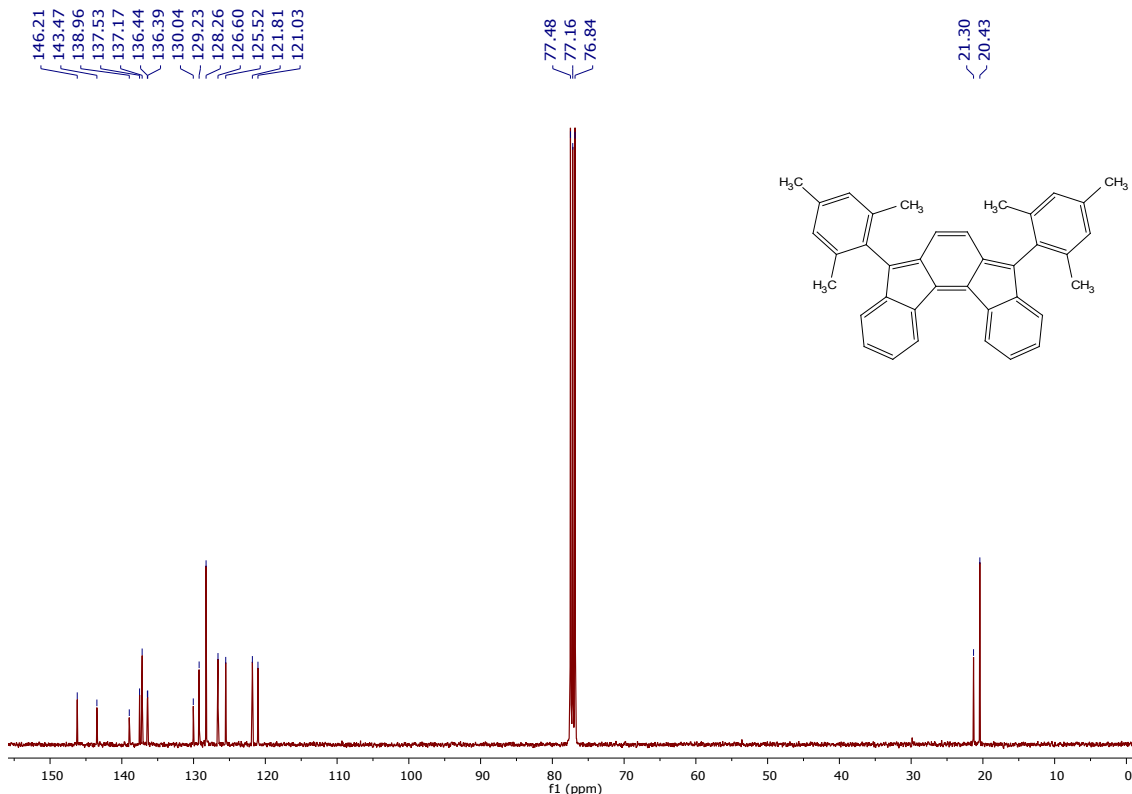


Fig. S11 ^{13}C NMR spectrum of **3** (in CDCl_3 , 100 MHz).

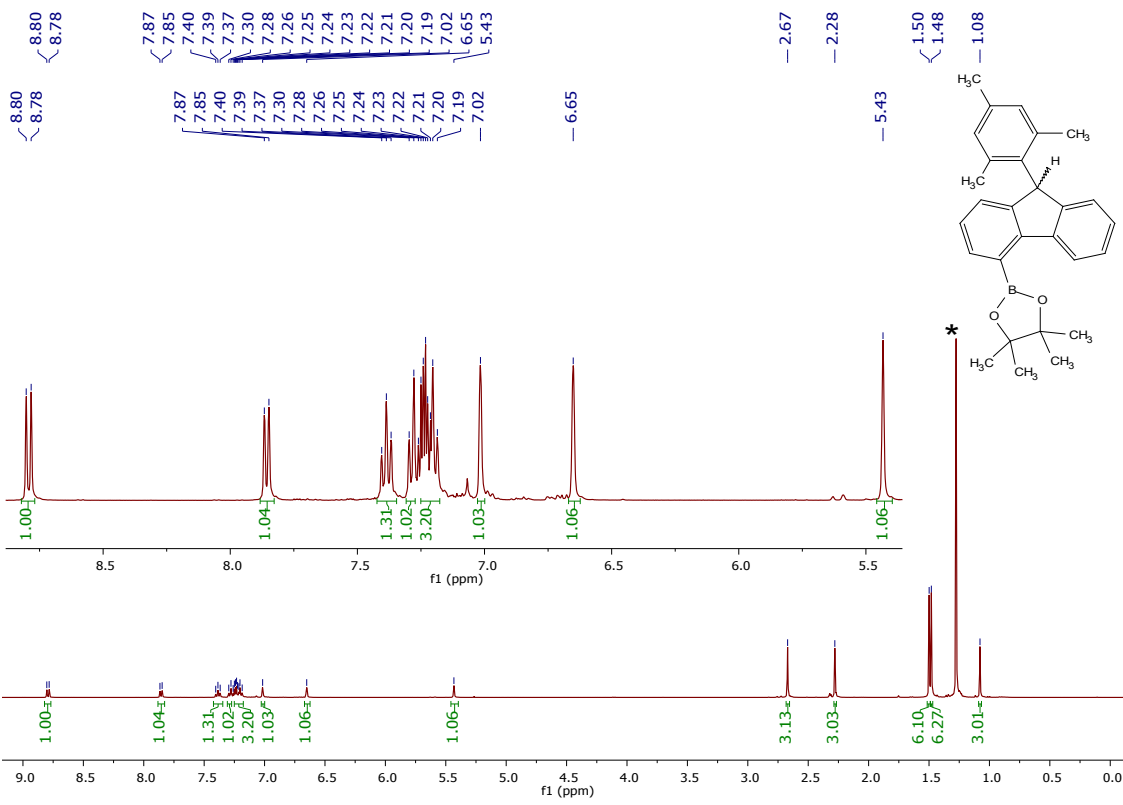


Fig. S13 ^{13}C NMR spectrum of **15** (in CDCl_3 , 100 MHz). * B_2Pin_2 impurity.

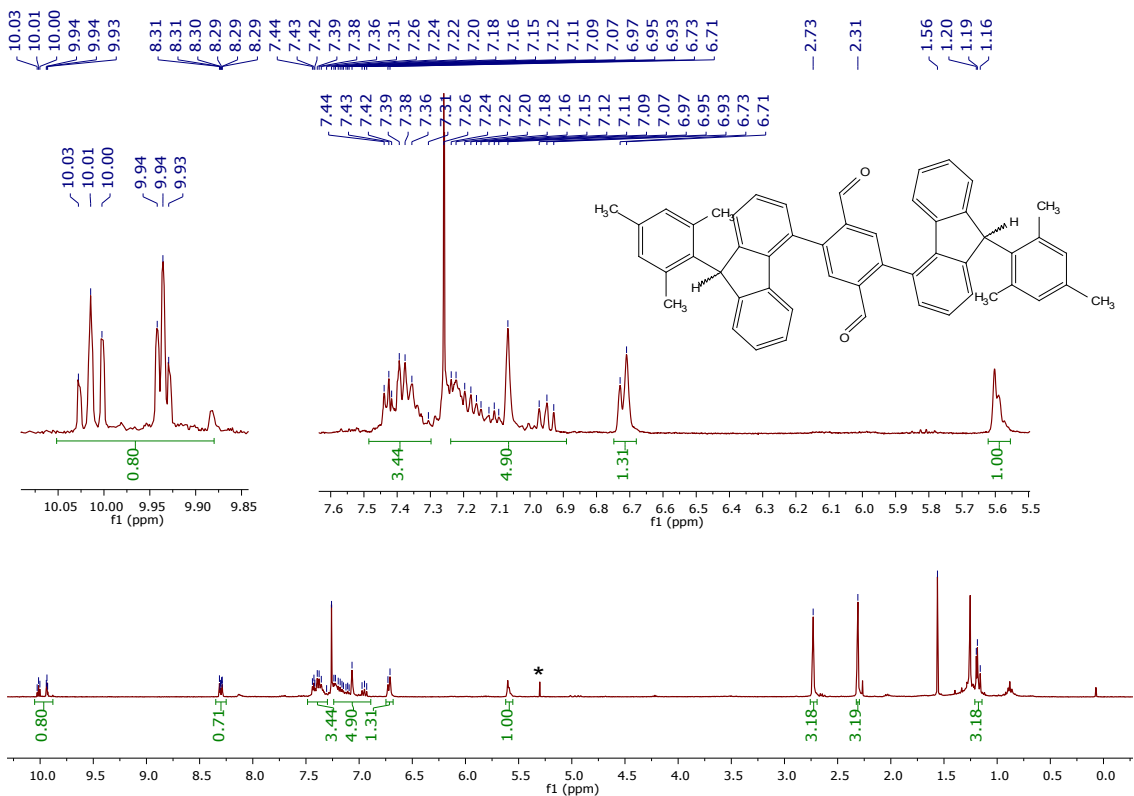


Fig. S14 ^1H NMR spectrum of **17** (in CDCl_3 , 400 MHz). * CH_2Cl_2 impurity.

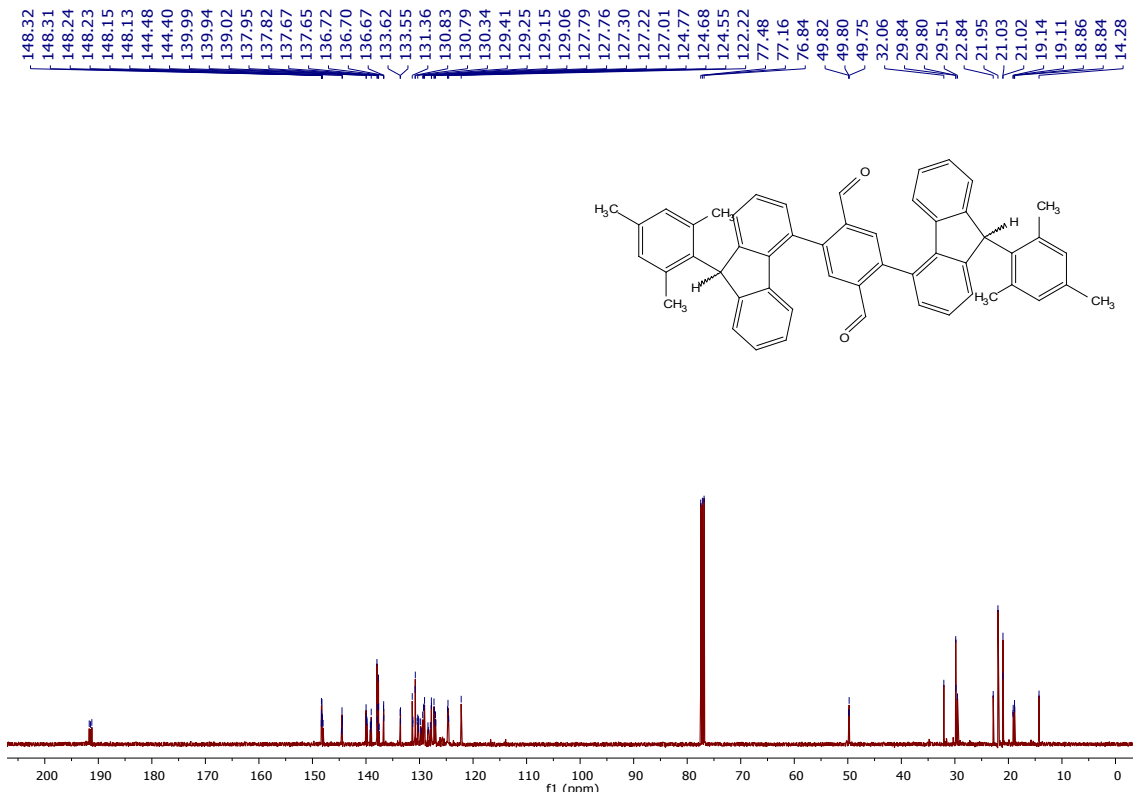


Fig. S15 ^{13}C NMR spectrum of **17** (in CDCl_3 , 100 MHz).

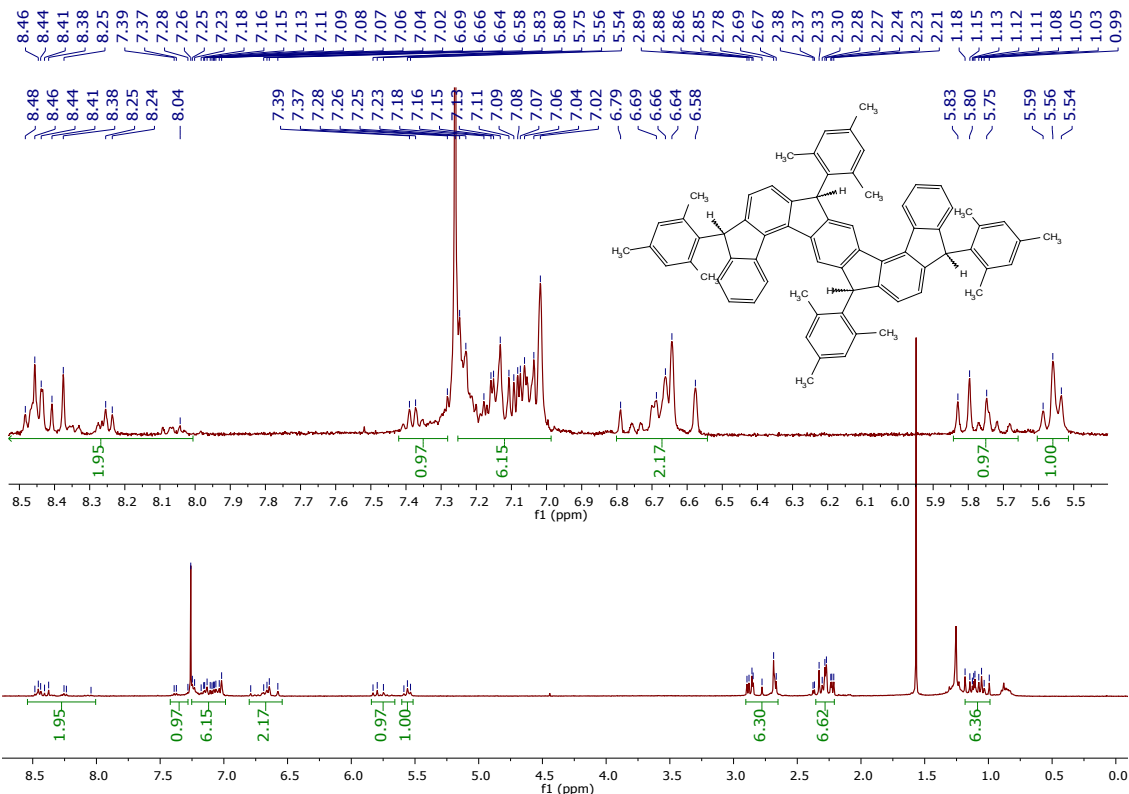


Fig. S16 ^1H NMR spectrum of **19** (in CDCl_3 , 400 MHz).

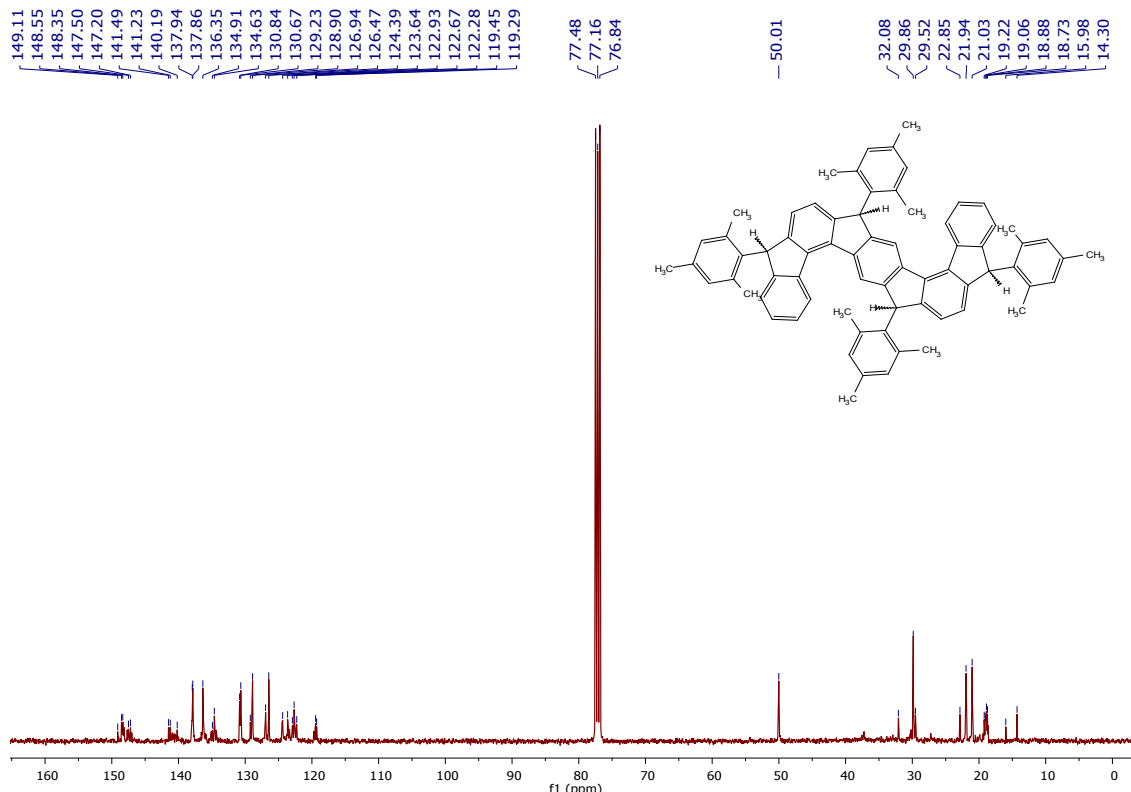


Fig. S17 ^{13}C NMR spectrum of **19** (in CDCl_3 , 100 MHz).

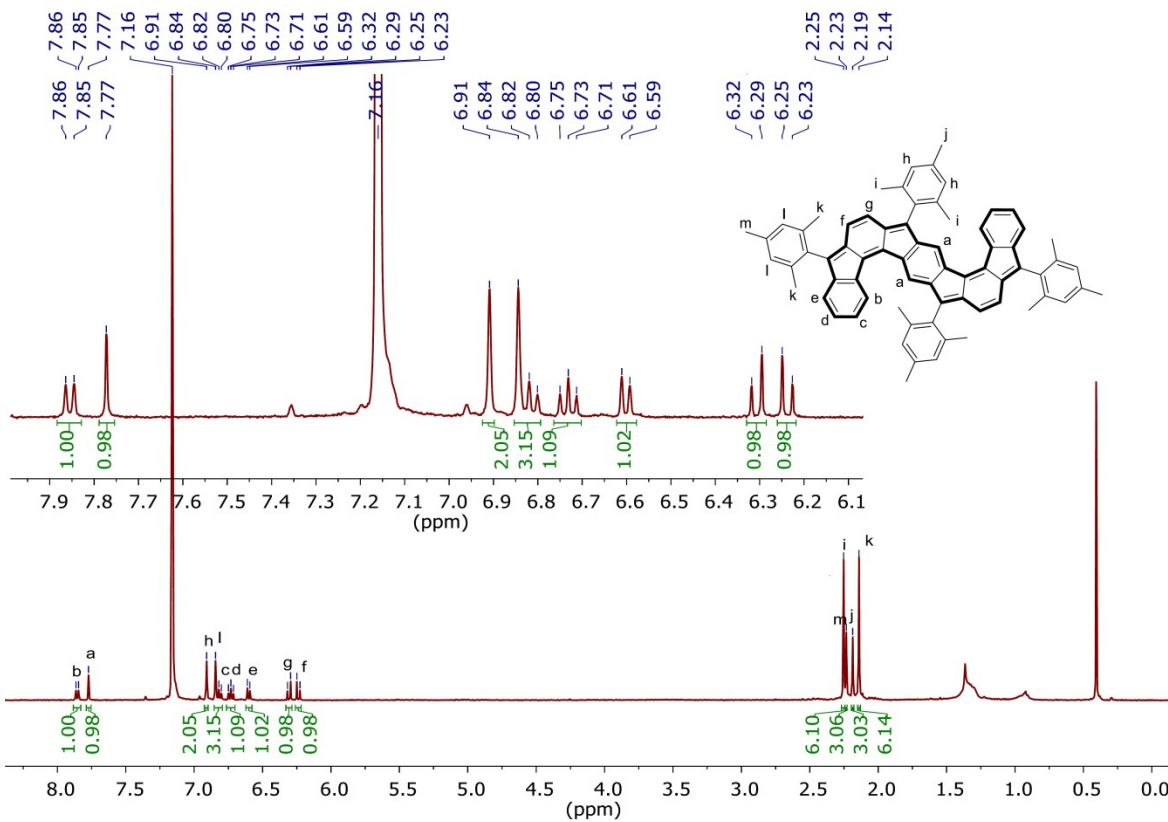


Fig. S18 ¹H NMR spectrum of **4** (in C_6D_6 , 400 MHz). H_2O at δ 0.40 ppm.

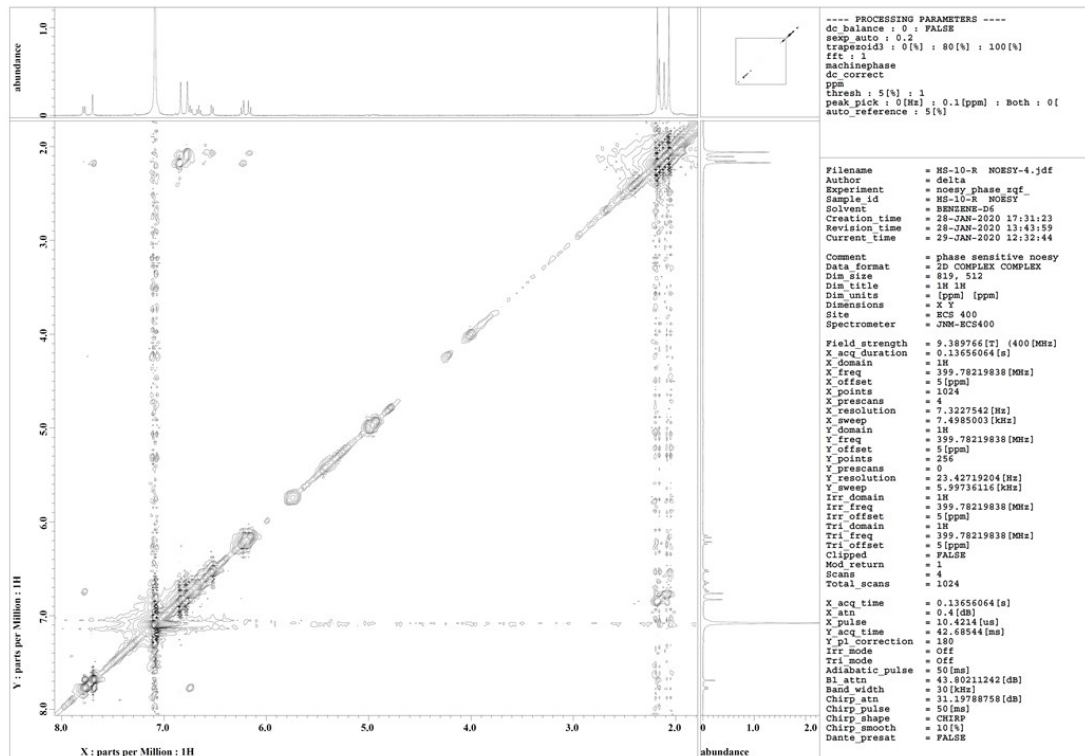


Fig. S19 ¹H-¹H NOESY, full spectrum of **4** in C_6D_6 .

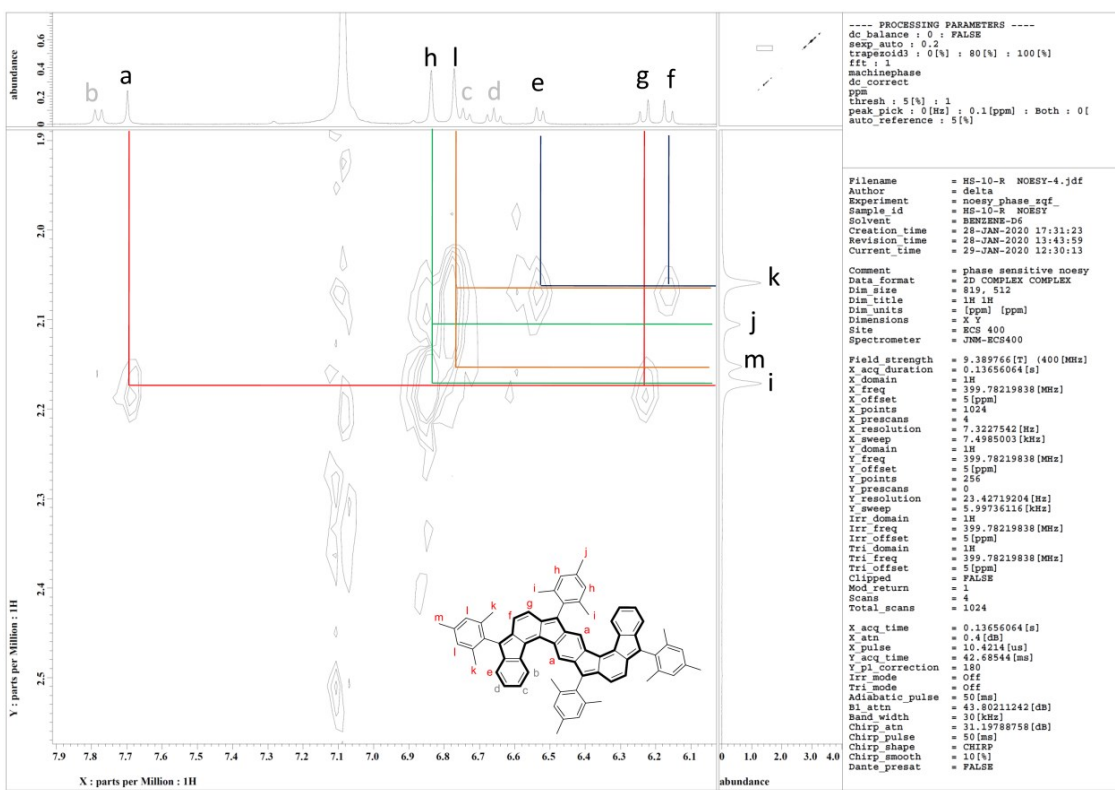


Fig. S20 Expanded ^1H - ^1H NOESY (aromatic vs aliphatic region) spectrum of 4.

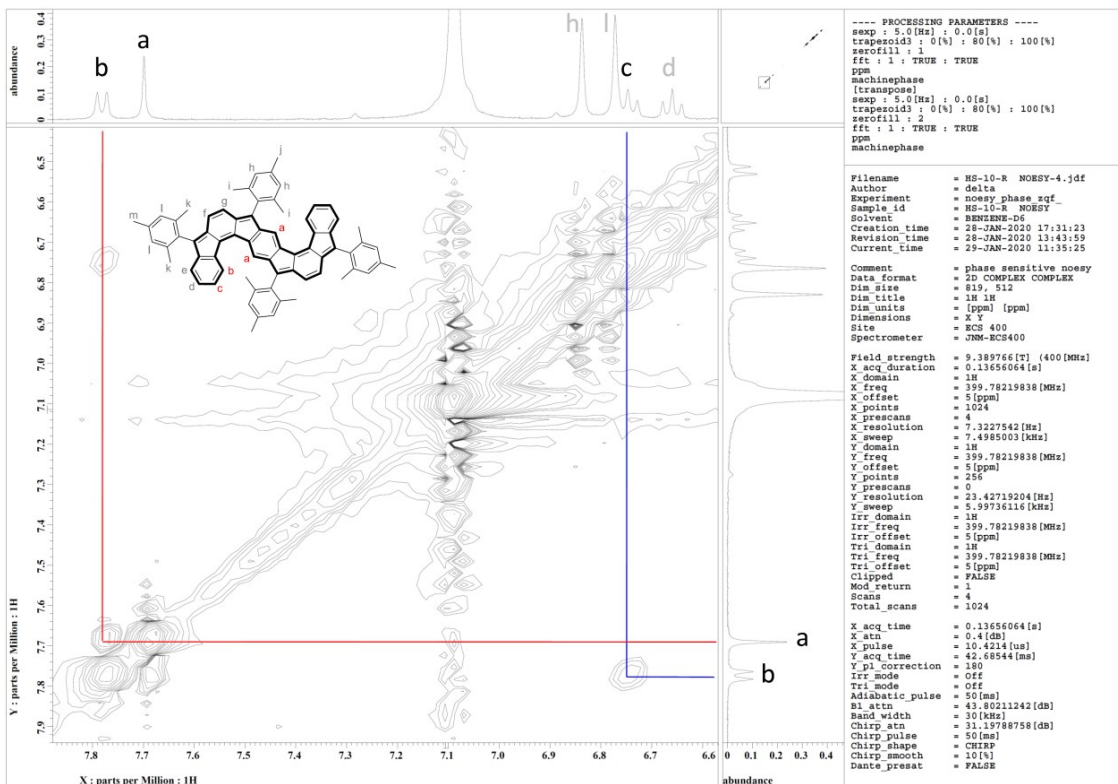


Fig. S21 Expanded ^1H - ^1H NOESY (aromatic vs aromatic region) spectrum of 4.

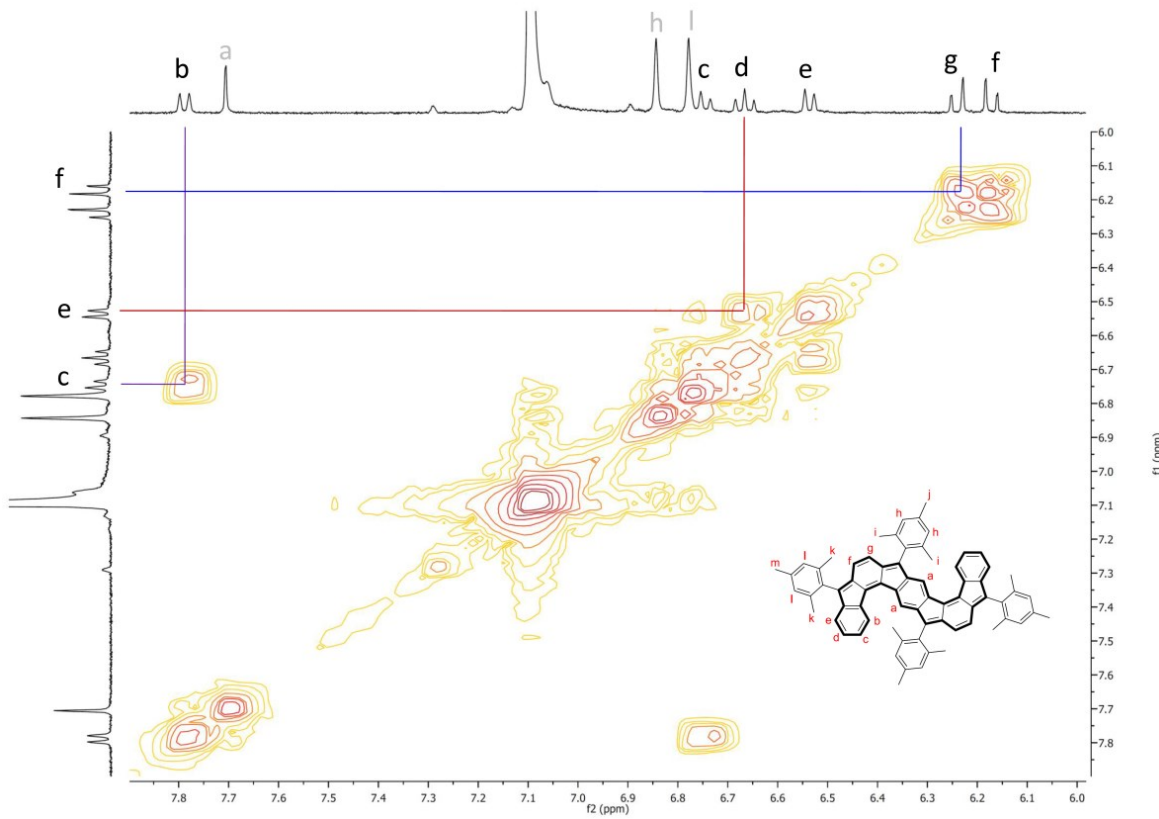


Fig. S22 ^1H - ^1H COSY spectrum of **4** in C_6D_6 .

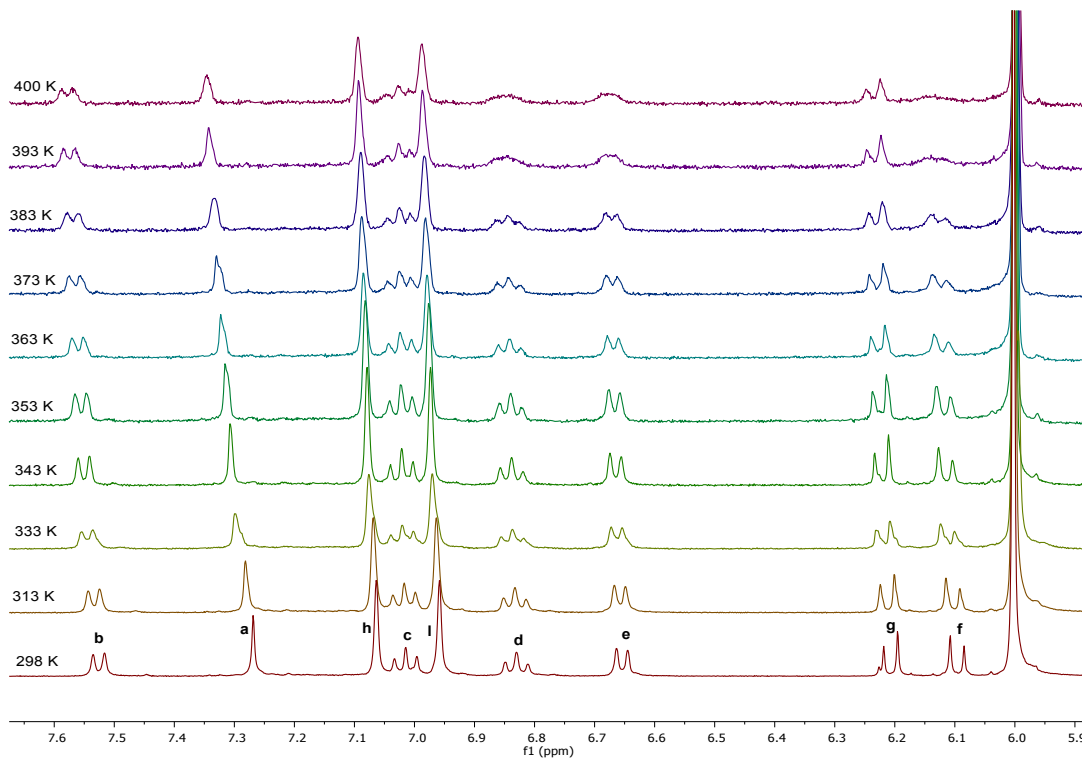


Fig. S23 Variable temperature ^1H NMR spectrum of **4** (in $\text{C}_2\text{D}_2\text{Cl}_4$, 400 MHz).

3. DFT Calculations

Density functional theory calculations were performed with Gaussian 09 package using a high performance computing cluster facility of IIT Ropar, utilizing both the B3LYP and CAM-B3LYP (restricted and unrestricted) level of theory with basis set 6-31G(d,p), in the gas phase.¹ NICS(1)zz values were estimated at the same levels using the standard GIAO procedure. Excitation energy was computed using time-dependent density functional theory (same theory level) for the singlet closed shell optimized geometry. Molecular orbital contributions were determined using GaussSum 3.0 package.² Diradical (y_0) and tetraradical (y_1) character indices were determined on the basis of the HOMO/LUMO and HOMO-1/LUMO+1 occupation numbers in natural orbital analysis, for the unrestricted CAM-B3LYP/6-31G(d,p) optimized singlet geometry. The y is formally expressed as $y = 1 - (2T/(1 + T^2))$, where T is represented by using the occupation numbers of UCAM-B3LYP natural orbitals as: $T = (n_{\text{HOMO}} - n_{\text{LUMO}})/2$ for diradical and $T = (n_{\text{HOMO}-1} - n_{\text{LUMO}+1})/2$ for tetraradical. A molecule with $y = 0$ indicates a closed-shell structure, whereas a molecule with $0 < y < 1$ implies diradicaloid (diradical-like) or tetraradicaloid (tetraradical-like) structures.

Table S1. Relative energies of optimized geometries for **4** at B3LYP/6-31G(d,p) level.

	State	HF	Kcal/mol
4	Singlet Closed Shell	-2702.55611363	-1695853.961
	Singlet Open Shell	-2702.55611363	-1695853.961
	Triplet Open Shell	-2702.54645986	-1695847.904

$$\Delta E_{\text{T-CS}} = 6.05 \text{ kcal/mol}$$

Table S2. Relative energies of optimized geometries, and radical character index for **4** at CAM-B3LYP/6-31G(d,p) level.

	State	HF	Kcal/mol	y_0	y_1
4	Singlet Closed Shell	-2700.94911548	-1694869.879		
	Singlet Open Shell	-2700.94911546	-1694869.878	0.0052	0.0008
	Triplet Open Shell	-2700.94080361	-1694864.663		

$$\Delta E_{\text{T-CS}} = 5.21 \text{ kcal/mol}$$

3.1 TD-DFT Calculations:

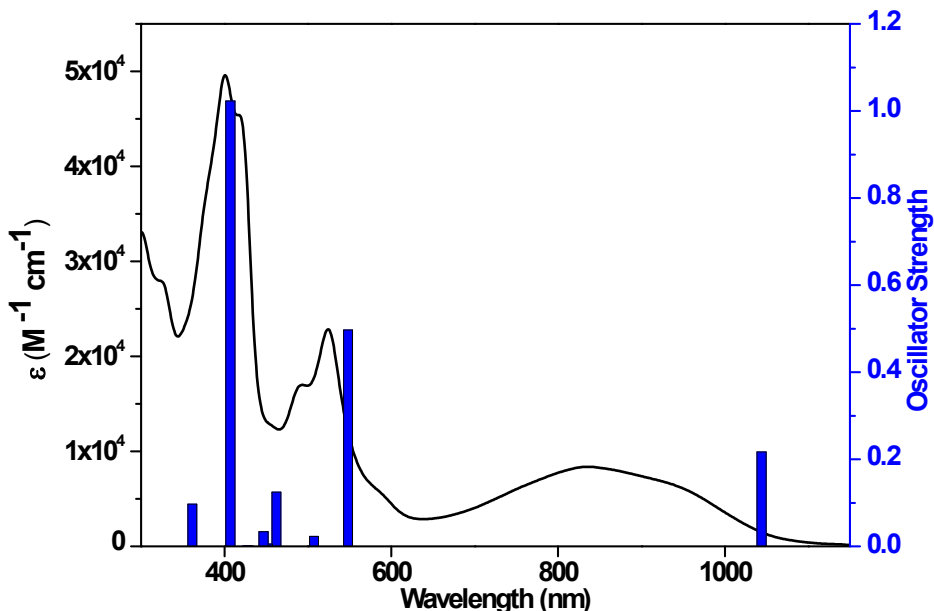


Fig. S24 Experimental absorption spectrum of **4**, against the simulated stick diagram showing oscillator strength at B3LYP/6-31G(d,p) level of theory.

Table S3. TD-DFT transitions at B3LYP/6-31G(d,p) level.

Wavelength (nm)	Osc. Strength (<i>f</i>)	Major contributions
1043.982	0.2171	HOMO->LUMO (95%)
694.5845	0	H-1->LUMO (95%)
663.5448	0	HOMO->L+1 (93%)
548.235	0.497	H-2->LUMO (83%)
507.276	0.0231	H-3->LUMO (90%)
464.6703	0	H-4->LUMO (92%)
462.3139	0.1248	H-1->L+1 (81%)
452.1144	0.0051	H-7->LUMO (14%), H-6->LUMO (81%)
451.1274	0	H-5->LUMO (93%)
446.7546	0.0337	H-7->LUMO (83%), H-6->LUMO (12%)
434.1153	0	H-11->LUMO (33%), H-10->LUMO (22%), H-2->L+1 (34%)
429.0972	0	H-11->LUMO (41%), H-10->LUMO (58%)
429.0229	0.0006	H-12->LUMO (95%)
427.2341	0	H-8->LUMO (91%)
426.9693	0.0005	H-9->LUMO (92%)
416.6527	0	H-11->LUMO (17%), H-10->LUMO (11%), H-2->L+1 (45%)
407.0633	1.0226	HOMO->L+2 (84%)
380.831	0	H-13->LUMO (24%), H-3->L+1 (64%)
367.8812	0	H-13->LUMO (69%), H-3->L+1 (27%)
361.4253	0.0973	H-4->L+1 (88%)

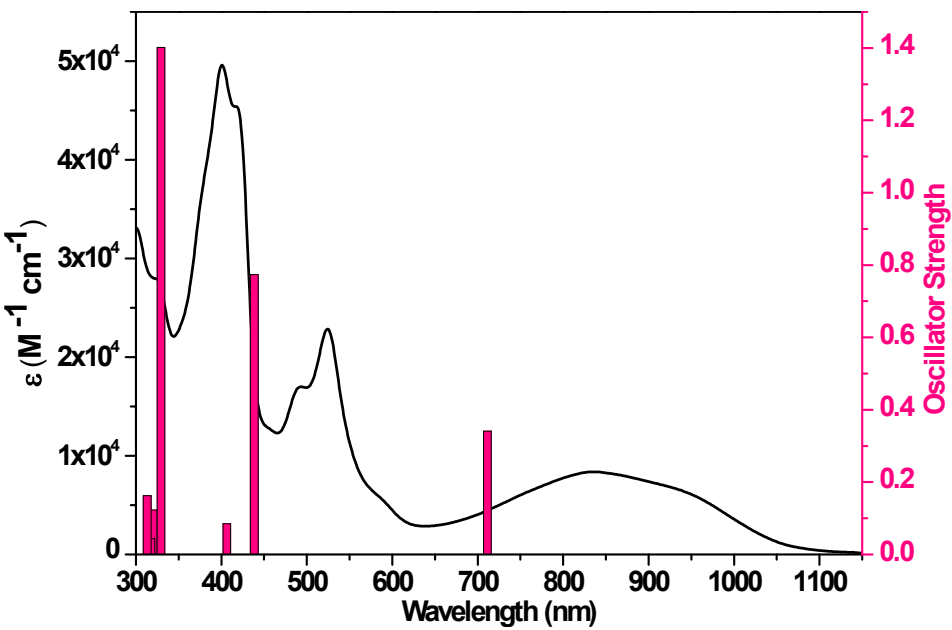


Fig. S25 Experimental absorption spectrum of **4**, against the simulated stick diagram showing oscillator strength at CAM-B3LYP/6-31G(d,p) level of theory.

Table S4. TD-DFT transitions at CAM-B3LYP/6-31G(d,p) level.

Wavelength (nm)	Osc. Strength (<i>f</i>)	Major contributions
711.4031	0.3411	HOMO->LUMO (86%)
544.838	0	H-1->LUMO (51%), HOMO->L+1 (36%)
438.4755	0.7732	H-2->LUMO (79%)
418.9051	0	H-3->L+1 (10%), H-1->LUMO (35%), HOMO->L+1 (46%)
406.3296	0.0851	H-3->LUMO (67%), H-1->L+1 (16%)
361.9106	0	H-8->LUMO (10%), H-4->LUMO (44%), H-2->L+1 (21%) H-13->LUMO (13%), H-4->LUMO (16%), H-3->L+1 (12%), H-2-
336.9112	0	>L+1 (38%), HOMO->L+1 (10%)
329.2875	1.4014	HOMO->L+2 (80%)
320.1636	0.1232	H-7->LUMO (19%), H-6->LUMO (44%), H-1->L+1 (11%)
318.9692	0	H-6->L+1 (20%), H-5->LUMO (74%) H-7->LUMO (23%), H-6->LUMO (29%), H-5->L+1 (10%), H-1-
317.6698	0.0435	>L+1 (21%)
315.4792	0	H-8->LUMO (63%), H-7->L+1 (10%), H-4->LUMO (14%)
313.0892	0.1621	H-7->LUMO (41%), H-1->L+1 (38%)
293.7506	0.0016	H-12->LUMO (80%)
293.3267	0	H-11->LUMO (93%)
291.7667	0.0211	H-14->LUMO (12%), H-10->LUMO (54%), H-9->L+1 (13%)
291.5814	0	H-10->L+1 (16%), H-9->LUMO (75%)
290.0195	0.0144	H-14->LUMO (25%), H-10->LUMO (26%)
289.4981	0	H-1->L+2 (39%), HOMO->L+3 (32%)
285.0847	0	H-13->LUMO (44%), H-2->L+1 (13%)

Table S5. Summary of experimental and theoretical HOMO-LUMO energy levels.

Compound	HOMO (eV)	LUMO (eV)	E_g^{DFT} (eV)	E_g^{EC} (eV)	E_g^{opt} (eV)
4	-4.89^{Exp}	-3.52^{Exp}			
	-4.54^{B3LYP}	-2.97^{B3LYP}	1.57^{B3LYP}		
	$-5.74^{\text{CAM-B3LYP}}$	$-1.94^{\text{CAM-B3LYP}}$	$3.80^{\text{CAM-B3LYP}}$	1.37	1.15

E_g^{DFT} = Theoretical HOMO-LUMO energy gap (from closed-shell geometry), E_g^{EC} = Electrochemical HOMO-LUMO energy gap, E_g^{opt} = Optical HOMO-LUMO energy gap.

It is evident from computational calculations that CAM-B3LYP/6-31G(d,p) may overestimate the HOMO-LUMO gap, and hence the HOMO to LUMO electronic absorption maximum is underestimated. Therefore, B3LYP/6-31G(d,p) level was used for optimization of **4** as well as the TD-DFT calculations. However, the three major transitions (highlighted in blue and pink in Table S3 and Table S4) for **4** are well reproduced by both the level of theories. The deviations from experimental spectrum may originate due to the polarization effects, and the solvent polarity.

3.2 Frontier Molecular Orbitals:

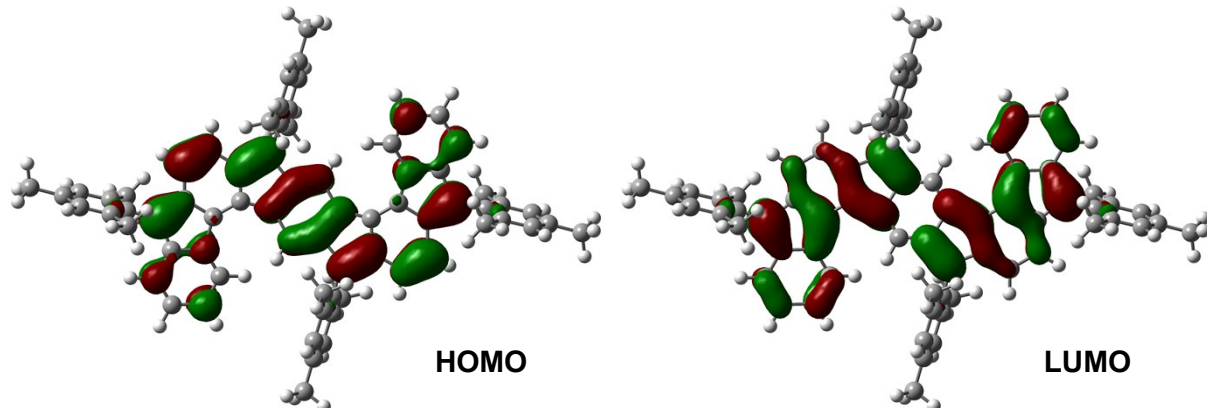
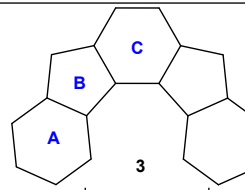
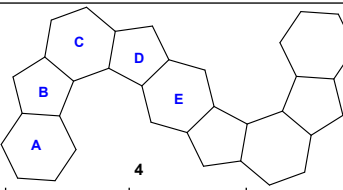


Fig. S26 Frontier molecular orbital profiles for **4**.

3.3 NICS(1)zz and HOMA Indices:

Table S6. NICS(1)zz and HOMA³ values of each ring for the mesityl-substituted **3** and **4**.

Compounds	 3			 4				
Rings	A	B	C	A	B	C	D	E
B3LYP/6-31G(d,p)								
NICS(1)zz	-13.30	19.29	8.17	-12.18	20.45	8.09	21.09	-0.33
HOMA	0.92	-0.22	0.05	0.91	-0.21	0.10	-0.12	0.85
CAM-B3LYP/6-31G(d,p)								
NICS(1)zz	-17.99	14.39	7.41	-17.35	15.86	7.85	16.25	-8.97
HOMA	0.96	-0.23	-0.06	0.96	-0.24	-0.04	-0.17	0.93

4. Single Crystal Data

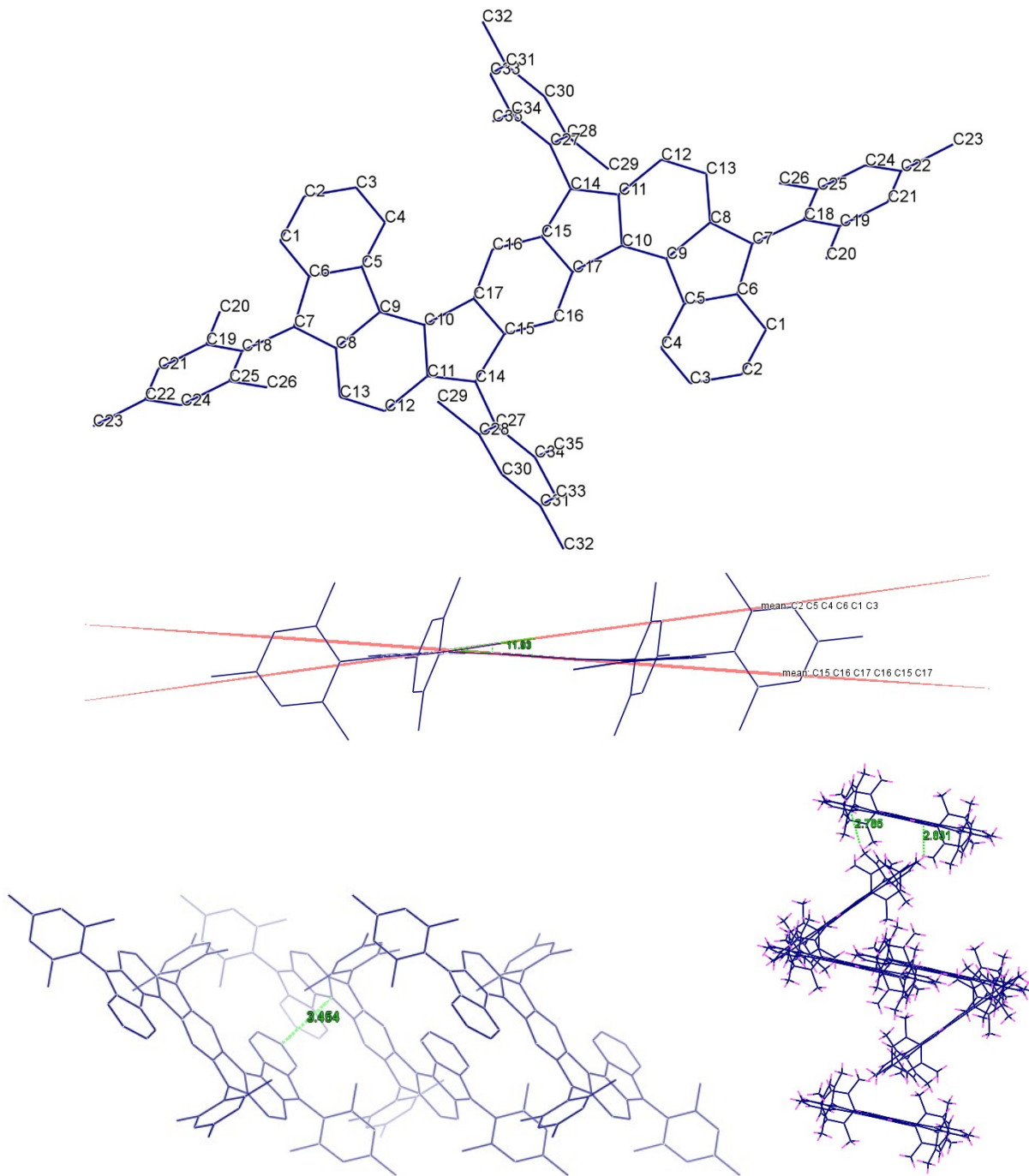


Fig. S27 Crystal structure of **4** with labels (upper row image). The terminal phenyl ring is deviated from central (core) phenyl ring by 11.93° due to steric congestion in the cove-like region between two hydrogens in close proximity (middle row image). The shortest interplanar C-C contact was found as 3.454 Å (left image, last row), and the intermolecular [C-H... π] interactions (2.831/2.785 Å) (right image, last row).

Table S7. Crystal data and structure refinement for **4**.

CCDC No.	2011386
Empirical formula	C ₇₀ H ₅₈
Formula weight	899.16
Temperature	100(2) K
Wavelength	0.71073 Å
Crystal system	Monoclinic
Space group	C2/c
Unit cell dimensions	a = 28.3914(11) Å α= 90°. b = 12.6728(4) Å β= 98.2380(10)°. c = 15.8260(6) Å γ = 90°.
Volume	5635.4(4) Å ³
Z	4
Density (calculated)	1.060 Mg/m ³
Absorption coefficient	0.060 mm ⁻¹
F(000)	1912
Crystal size	0.256 x 0.246 x 0.065 mm ³
Theta range for data collection	2.251 to 28.139°.
Index ranges	-36<=h<=37, -16<=k<=16, -20<=l<=20
Reflections collected	36309
Independent reflections	6877 [R(int) = 0.0805]
Completeness to theta = 25.242°	99.8 %
Absorption correction	Semi-empirical from equivalents
Max. and min. transmission	0.996 and 0.985
Refinement method	Full-matrix least-squares on F ²
Data / restraints / parameters	6877 / 0 / 322
Goodness-of-fit on F ²	1.022
Final R indices [I>2sigma(I)]	R1 = 0.0616, wR2 = 0.1574
R indices (all data)	R1 = 0.0930, wR2 = 0.1737
Extinction coefficient	n/a
Largest diff. peak and hole	0.301 and -0.240 e.Å ⁻³

Table S8. Bond lengths [\AA] and angles [$^\circ$] for **4**.

C(1)-C(6)	1.382(2)
C(1)-C(2)	1.391(3)
C(1)-H(1)	0.9300
C(2)-C(3)	1.379(3)
C(2)-H(2)	0.9300
C(3)-C(4)	1.394(2)
C(3)-H(3)	0.9300
C(4)-C(5)	1.381(2)
C(4)-H(4)	0.9300
C(5)-C(6)	1.421(2)
C(5)-C(9)	1.483(2)
C(6)-C(7)	1.460(2)
C(7)-C(8)	1.372(2)
C(7)-C(18)	1.479(2)
C(8)-C(13)	1.425(2)
C(8)-C(9)	1.470(2)
C(9)-C(10)	1.365(2)
C(10)-C(17)#1	1.473(2)
C(10)-C(11)	1.475(2)
C(11)-C(14)	1.373(2)
C(11)-C(12)	1.428(2)
C(12)-C(13)	1.352(2)
C(12)-H(12)	0.9300
C(13)-H(13)	0.9300
C(14)-C(15)	1.456(2)
C(14)-C(27)	1.479(2)
C(15)-C(16)	1.394(2)
C(15)-C(17)#1	1.417(2)
C(16)-C(17)	1.384(2)
C(16)-H(16)	0.9300
C(18)-C(19)	1.394(3)
C(18)-C(25)	1.396(2)
C(19)-C(21)	1.390(3)
C(19)-C(20)	1.503(3)

C(20)-H(20A)	0.9600
C(20)-H(20B)	0.9600
C(20)-H(20C)	0.9600
C(21)-C(22)	1.370(3)
C(21)-H(21)	0.9300
C(22)-C(24)	1.384(3)
C(22)-C(23)	1.511(3)
C(23)-H(23A)	0.9600
C(23)-H(23B)	0.9600
C(23)-H(23C)	0.9600
C(24)-C(25)	1.392(3)
C(24)-H(24)	0.9300
C(25)-C(26)	1.503(3)
C(26)-H(26A)	0.9600
C(26)-H(26B)	0.9600
C(26)-H(26C)	0.9600
C(27)-C(28)	1.401(3)
C(27)-C(34)	1.401(3)
C(28)-C(30)	1.391(3)
C(28)-C(29)	1.507(3)
C(29)-H(29A)	0.9600
C(29)-H(29B)	0.9600
C(29)-H(29C)	0.9600
C(30)-C(31)	1.381(3)
C(30)-H(30)	0.9300
C(31)-C(33)	1.379(3)
C(31)-C(32)	1.514(3)
C(32)-H(32A)	0.9600
C(32)-H(32B)	0.9600
C(32)-H(32C)	0.9600
C(33)-C(34)	1.391(3)
C(33)-H(33)	0.9300
C(34)-C(35)	1.498(3)
C(35)-H(35A)	0.9600
C(35)-H(35B)	0.9600
C(35)-H(35C)	0.9600

C(6)-C(1)-C(2)	118.68(16)
C(6)-C(1)-H(1)	120.7
C(2)-C(1)-H(1)	120.7
C(3)-C(2)-C(1)	120.45(17)
C(3)-C(2)-H(2)	119.8
C(1)-C(2)-H(2)	119.8
C(2)-C(3)-C(4)	121.03(18)
C(2)-C(3)-H(3)	119.5
C(4)-C(3)-H(3)	119.5
C(5)-C(4)-C(3)	119.77(16)
C(5)-C(4)-H(4)	120.1
C(3)-C(4)-H(4)	120.1
C(4)-C(5)-C(6)	118.61(15)
C(4)-C(5)-C(9)	134.73(15)
C(6)-C(5)-C(9)	106.63(14)
C(1)-C(6)-C(5)	121.40(16)
C(1)-C(6)-C(7)	129.45(15)
C(5)-C(6)-C(7)	109.13(14)
C(8)-C(7)-C(6)	108.39(14)
C(8)-C(7)-C(18)	125.50(16)
C(6)-C(7)-C(18)	126.10(15)
C(7)-C(8)-C(13)	128.65(15)
C(7)-C(8)-C(9)	109.71(14)
C(13)-C(8)-C(9)	121.64(14)
C(10)-C(9)-C(8)	118.20(14)
C(10)-C(9)-C(5)	135.72(14)
C(8)-C(9)-C(5)	106.05(13)
C(9)-C(10)-C(17)#1	135.09(14)
C(9)-C(10)-C(11)	118.90(14)
C(17)#1-C(10)-C(11)	105.99(13)
C(14)-C(11)-C(12)	129.10(14)
C(14)-C(11)-C(10)	109.57(13)
C(12)-C(11)-C(10)	121.32(14)
C(13)-C(12)-C(11)	119.58(15)
C(13)-C(12)-H(12)	120.2

C(11)-C(12)-H(12)	120.2
C(12)-C(13)-C(8)	120.22(15)
C(12)-C(13)-H(13)	119.9
C(8)-C(13)-H(13)	119.9
C(11)-C(14)-C(15)	108.14(13)
C(11)-C(14)-C(27)	128.91(14)
C(15)-C(14)-C(27)	122.89(14)
C(16)-C(15)-C(17)#1	122.41(14)
C(16)-C(15)-C(14)	128.16(14)
C(17)#1-C(15)-C(14)	109.38(13)
C(17)-C(16)-C(15)	118.26(14)
C(17)-C(16)-H(16)	120.9
C(15)-C(16)-H(16)	120.9
C(16)-C(17)-C(15)#1	119.31(14)
C(16)-C(17)-C(10)#1	133.74(14)
C(15)#1-C(17)-C(10)#1	106.86(13)
C(19)-C(18)-C(25)	119.85(16)
C(19)-C(18)-C(7)	119.54(15)
C(25)-C(18)-C(7)	120.58(16)
C(21)-C(19)-C(18)	119.21(17)
C(21)-C(19)-C(20)	120.90(18)
C(18)-C(19)-C(20)	119.89(16)
C(19)-C(20)-H(20A)	109.5
C(19)-C(20)-H(20B)	109.5
H(20A)-C(20)-H(20B)	109.5
C(19)-C(20)-H(20C)	109.5
H(20A)-C(20)-H(20C)	109.5
H(20B)-C(20)-H(20C)	109.5
C(22)-C(21)-C(19)	122.20(19)
C(22)-C(21)-H(21)	118.9
C(19)-C(21)-H(21)	118.9
C(21)-C(22)-C(24)	117.75(17)
C(21)-C(22)-C(23)	121.6(2)
C(24)-C(22)-C(23)	120.7(2)
C(22)-C(23)-H(23A)	109.5
C(22)-C(23)-H(23B)	109.5

H(23A)-C(23)-H(23B)	109.5
C(22)-C(23)-H(23C)	109.5
H(23A)-C(23)-H(23C)	109.5
H(23B)-C(23)-H(23C)	109.5
C(22)-C(24)-C(25)	122.39(18)
C(22)-C(24)-H(24)	118.8
C(25)-C(24)-H(24)	118.8
C(24)-C(25)-C(18)	118.56(18)
C(24)-C(25)-C(26)	121.16(18)
C(18)-C(25)-C(26)	120.28(17)
C(25)-C(26)-H(26A)	109.5
C(25)-C(26)-H(26B)	109.5
H(26A)-C(26)-H(26B)	109.5
C(25)-C(26)-H(26C)	109.5
H(26A)-C(26)-H(26C)	109.5
H(26B)-C(26)-H(26C)	109.5
C(28)-C(27)-C(34)	119.88(15)
C(28)-C(27)-C(14)	120.34(16)
C(34)-C(27)-C(14)	119.67(16)
C(30)-C(28)-C(27)	118.92(19)
C(30)-C(28)-C(29)	120.11(19)
C(27)-C(28)-C(29)	120.97(16)
C(28)-C(29)-H(29A)	109.5
C(28)-C(29)-H(29B)	109.5
H(29A)-C(29)-H(29B)	109.5
C(28)-C(29)-H(29C)	109.5
H(29A)-C(29)-H(29C)	109.5
H(29B)-C(29)-H(29C)	109.5
C(31)-C(30)-C(28)	122.1(2)
C(31)-C(30)-H(30)	119.0
C(28)-C(30)-H(30)	119.0
C(33)-C(31)-C(30)	118.07(18)
C(33)-C(31)-C(32)	120.7(2)
C(30)-C(31)-C(32)	121.2(2)
C(31)-C(32)-H(32A)	109.5
C(31)-C(32)-H(32B)	109.5

H(32A)-C(32)-H(32B)	109.5
C(31)-C(32)-H(32C)	109.5
H(32A)-C(32)-H(32C)	109.5
H(32B)-C(32)-H(32C)	109.5
C(31)-C(33)-C(34)	122.3(2)
C(31)-C(33)-H(33)	118.9
C(34)-C(33)-H(33)	118.9
C(33)-C(34)-C(27)	118.77(19)
C(33)-C(34)-C(35)	120.00(19)
C(27)-C(34)-C(35)	121.23(17)
C(34)-C(35)-H(35A)	109.5
C(34)-C(35)-H(35B)	109.5
H(35A)-C(35)-H(35B)	109.5
C(34)-C(35)-H(35C)	109.5
H(35A)-C(35)-H(35C)	109.5
H(35B)-C(35)-H(35C)	109.5

Symmetry transformations used to generate equivalent atoms:

#1 -x+3/2,-y+3/2,-z+2

5. References

1. Gaussian 09, Revision B.01, M. J. Frisch, G. W. Trucks, H. B. Schlegel, G. E. Scuseria, M. A. Robb, J. R. Cheeseman, G. Scalmani, V. Barone, B. Mennucci, G. A. Petersson, H. Nakatsuji, M. Caricato, X. Li, H. P. Hratchian, A. F. Izmaylov, J. Bloino, G. Zheng, J. L. Sonnenberg, M. Hada, M. Ehara, K. Toyota, R. Fukuda, J. Hasegawa, M. Ishida, T. Nakajima, Y. Honda, O. Kitao, H. Nakai, T. Vreven, J. A. Montgomery, Jr., J. E. Peralta, F. Ogliaro, M. Bearpark, J. J. Heyd, E. Brothers, K. N. Kudin, V. N. Staroverov, T. Keith, R. Kobayashi, J. Normand, K. Raghavachari, A. Rendell, J. C. Burant, S. S. Iyengar, J. Tomasi, M. Cossi, N. Rega, J. M. Millam, M. Klene, J. E. Knox, J. B. Cross, V. Bakken, C. Adamo, J. Jaramillo, R. Gomperts, R. E. Stratmann, O. Yazyev, A. J. Austin, R. Cammi, C. Pomelli, J. W. Ochterski, R. L. Martin, K. Morokuma, V. G. Zakrzewski, G. A. Voth, P. Salvador, J. J. Dannenberg, S. Dapprich, A. D. Daniels, O. Farkas, J. B. Foresman, J. V. Ortiz, J. Cioslowski and D. J. Fox, Gaussian, Inc., Wallingford CT, 2010.
2. N. M. O'Boyle, A. L. Tenderholt and K. M. Langner, *J. Comp. Chem.* 2008, **29**, 839-845.

3. J. Kruszewski and T.M. Krygowski, *Tetrahedron Lett.* 1972, **13**, 3839-3842.